

## **On the representation of hyetograph characteristics by stochastic rainfall models**

Demetris Koutsoyiannis and Nikos Mamassis

Department of Water Resources, Faculty of Civil Engineering,  
National Technical University, Athens, Greece

**Abstract.** Two stochastic models of the rainfall process, belonging to different categories, are compared in terms of how well they reproduce certain hyetograph characteristics. The first is the scaling model of storm hyetograph, which belongs to the category of storm-based models. The second is the Bartlett-Lewis rectangular pulse model, the most widespread among the category of point process models. The scaling model is further developed introducing one more parameter to better fit historical data. The Bartlett-Lewis model is theoretically studied to extract mathematical relationships for the intra-storm structure. The intercomparison is based on the storm hyetographs of a data set from Greece and another one from USA. The different storms are identified in each data set and classified according to their duration. Both models are fitted using the characteristics of storms. The comparison shows that the scaling model of storm hyetograph agrees well with the structure of historical hyetographs whereas the Bartlett-Lewis rectangular pulse model exhibits some discrepancies in either its original version or its random parameter version. However, it is shown that the performance of the Bartlett-Lewis model is significantly improved, and becomes comparable to that of the scaling model, by introducing a power-law dependence of its cell related parameters (duration and rate of arrivals) on the storm duration.

**Keywords.** Stochastic models; Rainfall; Storm; Hyetograph; Point process; Scaling.

## 1. Introduction

Stochastic rainfall models based on point processes, introduced in the 1980s (Waymire and Gupta, 1981a-b; Smith and Karr, 1983; Rodriguez-Iturbe et al., 1984, Foufoula-Georgiou and Lettenmaier, 1986; Guttorp, 1986), have been one of the most widespread and useful tools in analysis and modelling of rainfall. Among them, the cluster-based models (Rodriguez-Iturbe et al., 1987, 1988) such as the Neyman-Scott rectangular pulse model and the Bartlett-Lewis rectangular pulse model (especially the latter, see section 3) have offered a more accurate representation of rainfall and have become the most popular. In these models, storms arrive following a Poisson process and each storm gives rise to a cluster of rain cells with each cell having a random time location, duration and intensity. Several applications of these models have been made and much research resulting in improvements thereof has been conducted during the 1990s (Cowpertwait, 1991, 1998; Onof and Wheater, 1993, 1994; Onof et al., 1994; Bo and Islam, 1994; Velghe et al., 1994; Glasbey et al., 1995; Cowpertwait et al., 1996a, b; Khaliq and Cunnane, 1996; Gyasi-Agyei and Willgoose, 1997, 1999; Verhoest et al., 1997; Kakou, 1997; Gyasi-Agyei, 1999; Cameron et al., 2000; Koutsoyiannis and Onof, 2001).

It is known that some of the point process models suffer from an inability to describe the statistical structure of rainfall at a wide range of scales (e.g. Foufoula-Georgiou and Guttorp, 1986; Foufoula-Georgiou and Krajewski, 1995). In addition, they may not represent well the extreme rainfall events at a range of scales (e.g. Valdes et al., 1985, Verhoest et al., 1997; Cameron et al., 2000), although recent developments have mitigated this problem either by explicitly incorporating the process skewness into the parameter estimation procedure (Cowpertwait, 1998) or by implementing a disaggregation framework using historical daily rainfall data (Koutsoyiannis and Onof, 2001). These problems may arise from the fact that the model parameters do not necessarily represent actual physical quantities as they depend on the time scale that was chosen for their fitting (e.g. Foufoula-Georgiou and Guttorp, 1986; Valdes et al., 1985). Specifically, the model fitting is usually done in terms of some bulk statistical properties of the process in the entire time domain such as marginal moments and

autocorrelations in discrete time and the probability of dry intervals, without focus on the structure of the individual rainfall events.

More than a decade before the introduction and use of point process based rainfall models, other types of statistical representations of the rainfall process focusing on the rainfall events were devised. These ranged from empirical non-dimensionalised mass curves of storms (Huff, 1967) to more theoretically based stochastic models (Grace and Eagleson, 1966; Eagleson, 1970, 1978; Restrepo-Posada and Eagleson, 1982; Woolhiser and Osborn, 1985; Marien and Vandewiele, 1986; Koutsoyiannis, 1988, 1994; Koutsoyiannis and Xanthopoulos, 1990). A more sophisticated model of this category, termed scaling model of storm hyetograph, was proposed by Koutsoyiannis and Foufoula-Georgiou (1993). This is a simple scaling stochastic model of instantaneous rainfall intensities based on an observed scale-invariance of dimensionless rainfall with storm duration (see also section 2). The common characteristic of these approaches was the focusing of the models on the rainy period rather than the description of the process in the entire time domain. To this aim, they had to partition the time domain into rainy and dry periods, consider each rainy period as a storm with certain characteristics such as total duration and depth, and study the internal structure of the storm. In comparison with point process models, the storm-based models may sometimes have less elegant mathematical basis, but they may describe better some properties of the rainfall process, particularly the intra-storm structure (we will discuss this later). Although storm-based models are dealing with storms only, it is not difficult to combine them with a stochastic scheme describing storm arrivals so as to compose a model for the entire time domain. For example, Koutsoyiannis and Pachakis (1996) combined the scaling model of storm hyetograph with an alternating renewal model to simulate completely the rainfall process.

A specific difficulty with storm-based models is that they require a definition of a storm in a manner that a storm can be identifiable from a rainfall record. This is not as easy as it may seem at first glance, as a storm may contain periods with zero rainfall. Periods of zero rainfall are contained in 'storms' of point process models (e.g., periods not covered by storm cells), too, but in this case there is no need that the abstract 'storms' of the models correspond to

actual storms of a rainfall time series. (As we discussed above, the fitting of point processes is done for the entire time domain). The usual convention in storm-based models is to consider all zero rainfall periods that are shorter than a specified limit (the separation time) as belonging to a storm, whereas longer zero rainfall periods are assumed to separate different storms. Huff (1967) assumed a value of 6 hours for this separation time. Restrepo-Posada and Eagleson (1982) assumed that this time must be defined in a manner that consecutive storms are statistically independent events and developed a statistical procedure to determine it. In the same lines, Koutsoyiannis and Xanthopoulos (1990) used a criterion based on the Kolmogorov-Smirnov test and found the separation time value in the range 5-7 hours using Greek rainfall data.

Despite of subjectivity in constructing a series of storm hyetographs from a continuous rainfall record, the different hyetographs, once identified, contain important information on the structure of the actual rainfall process. Their systematic study may be directly useful to engineering applications like design storm estimation. In addition, it is useful in rainfall modelling as it may reveal how well certain characteristics of the hyetographs can be reproduced by a stochastic model of rainfall. Thus, it can serve as a basis in building an appropriate stochastic model, improving the structure of an existing model, or choosing the most suitable among different rainfall models.

Such a study of the structure of rainfall event hyetographs is attempted in this paper. This study is used to assess how well the structure of hyetographs is described by existing stochastic models. For comparison, one representative model of each of the two model categories is chosen. The scaling model of storm hyetograph is chosen for the category of storm-based models (section 2) and is further developed introducing one more parameter to better fit historical data. The Bartlett-Lewis rectangular pulse model is chosen for the point process category (section 3) and is theoretically studied to extract mathematical relationships for the intra-storm structure. A data set from Greece and another one from the USA (section 4) are used for the study and comparisons. The comparison reveals that the scaling model of storm hyetograph captures well the structure of historical hyetographs whereas the Bartlett-Lewis rectangular pulse model may exhibit some discrepancies (section 5). Ways to improve

the Bartlett-Lewis model performance, by introducing dependence of its cell related parameters (duration and rate of arrivals) on the storm duration, are also discussed. The paper concludes by indicating the further research required to implement the studied adaptations into an operational model (section 6). To increase readability the mathematical derivations have been excluded from the text and are put separately in appendices (A1-A4).

## 2. The Scaling Model of Storm Hyetograph

Let  $D$  denote the duration of a storm and  $\Xi(t | D)$  the instantaneous rainfall intensity at time  $t$  within the storm duration ( $0 \leq t \leq D$ ). The scaling model of storm hyetograph is based on the scaling hypothesis, illustrated in the schematic of Figure 1 (Koutsoyiannis and Foufoula-Georgiou, 1993), i.e.,

$$\{\Xi(t | D)\} \stackrel{d}{=} \{\lambda^{-\kappa} \Xi(\lambda t | \lambda D)\} \quad (1)$$

where  $\kappa$  is a scaling exponent,  $\lambda$  is any positive real number and the symbol  $\stackrel{d}{=}$  denotes equality in distribution. A secondary hypothesis is the weak stationarity (stationarity within the storm), which results in

$$E[\Xi(t | D)] = c_1 D^\kappa \quad (2)$$

$$R_\Xi(\tau | D) := E[\Xi(t | D) \Xi(t + \tau | D)] = \psi(\tau / D) D^{2\kappa} \quad (3)$$

where  $E[ \ ]$  denotes expectation,  $c_1$  is a parameter ( $c_1 > 0$ ) and  $\psi(\tau / D)$  is a function to be specified. In this paper we specify this function as

$$\psi(\tau / D) = \alpha \left[ \left| \frac{\tau}{D} \right|^{-\beta} - \zeta \right] \quad (4)$$

where  $\alpha$ ,  $\beta$ ,  $\zeta$  are parameters ( $\alpha > 0$ ,  $0 < \beta < 1$ ,  $\zeta < 1$ ). This expression is slightly modified in comparison with the original expression by Koutsoyiannis and Foufoula-Georgiou (1993) as it contains the additional parameter  $\zeta$ . This additional parameter has been proven to improve

model fits to real world data. Note that the variance of the instantaneous process is infinite since  $\psi(\tau / D)$  tends to infinity as time lag  $\tau$  tends to zero.

Moving from continuous time to discrete time, we divide the time domain into  $k$  intervals of length  $\Delta = \delta D$  assuming for simplicity that  $k = 1 / \delta = D / \Delta$  is integer. Let  $Y_i$  denote the incremental rainfall depth at time interval  $i$  ( $1 \leq i \leq k$ ). The first- and second-order moments of the incremental depths are

$$E[Y_i] = c_1 D^{1+\kappa} \delta \quad (5)$$

$$\text{Var}[Y_i] = D^{2(1+\kappa)} \delta^2 \frac{(c_1^2 + c_2)(\delta^{-\beta} - \varepsilon) - c_1^2(1 - \varepsilon)}{1 - \varepsilon} \quad (6)$$

$$\text{Cov}[Y_i, Y_{i+m}] = D^{2(1+\kappa)} \delta^2 \frac{(c_1^2 + c_2)[\delta^{-\beta} f(m, \beta) - \varepsilon] - c_1^2(1 - \varepsilon)}{1 - \varepsilon} \quad (7)$$

so that

$$\text{Corr}[Y_i, Y_{i+m}] = \frac{(c_1^2 + c_2)[\delta^{-\beta} f(m, \beta) - \varepsilon] - c_1^2(1 - \varepsilon)}{(c_1^2 + c_2)(\delta^{-\beta} - \varepsilon) - c_1^2(1 - \varepsilon)} \quad (8)$$

where

$$c_2 = \frac{\alpha(1 - \varepsilon)}{(1 - \beta)(1 - \beta/2)} - c_1^2 \quad (9)$$

$$\varepsilon = \zeta(1 - \beta)(1 - \beta/2) \quad (10)$$

and

$$f(m, \beta) = \begin{cases} \frac{1}{2}[(m-1)^{2-\beta} + (m+1)^{2-\beta}] - m^{2-\beta}, & m > 0 \\ 1, & m = 0 \end{cases} \quad (11)$$

These expressions are slightly different from the original ones due to the additional parameter  $\zeta$ . (To get the original expressions it suffices to set  $\zeta = 0$ ). Their derivation is given in

Appendix A1. The relevant statistics of the total depth,  $H$ , of the storm, directly obtained from (5) and (6) by setting  $\delta = 1$ , are

$$E[H] = c_1 D^{1+\kappa} \quad (12)$$

$$\text{Var}[H] = c_2 D^{2(1+\kappa)} \quad (13)$$

From the above equations we may observe the following:

1. The mean  $E[H]$  and the standard deviation  $\text{Std}[H]$ , if plotted on a log-log paper versus duration  $D$ , will be parallel straight lines with slope  $1 + \kappa$ . Usually  $\kappa$  is negative so that this slope is less than 1. Consequently, the coefficient of variation  $\text{CV}[H] := \text{Std}[H] / E[H]$  is constant, independent of  $D$ .
2. The same is true for the statistics of the incremental depths, i.e.,  $E[Y_i]$  and  $\text{Std}[Y_i]$  if the number of intervals  $k$  (and, consequently the dimensionless interval length  $\delta$ ) is constant. However, if we assume a constant interval length  $\Delta$ , the mean incremental depth becomes  $E[Y_i] = c_1 D^\kappa \Delta$ , which for negative  $\kappa$  is a decreasing function of  $D$ . The behaviour of  $\text{Std}[Y_i]$  is similar.
3. For large lag  $m$  the autocorrelation structure is long-memory structure due to the presence of the term  $f(m, \beta)$ . (This term characterises also the fractional Gaussian noise model.)
4. The lag-one autocorrelation coefficient is generally an increasing function of storm duration  $D$ .

The model includes five parameters in total: the scaling exponent  $\kappa$ , the mean value parameter  $c_1$ , the variance parameter  $c_2$  (or, equivalently,  $\alpha$ ) and the correlation decay parameters  $\beta$  and  $\zeta$ . The first two can be estimated by least squares from  $E[H] = c_1 D^{1+\kappa}$  using storm data classified according to duration. The third parameter can be estimated from  $c_2 = \text{Var}[H] / D^{2(1+\kappa)}$ . The remaining two parameters can be estimated by least squares from

$$\frac{\delta^{-\beta} - \varepsilon}{1 - \varepsilon} = \frac{E[Y_i^2] E^2[H]}{E^2[Y_i] E[H^2]} \quad (14)$$

in combination with (10). Equation (14) is derived by combining (5), (6), (12) and (13). Alternatively, the three parameters  $c_2$ ,  $\beta$  and  $\zeta$  can be estimated simultaneously by minimising the fitting error of the model in  $\text{Var}[H]$ ,  $\text{Var}[Y]$  and  $\text{Corr}[Y_i, Y_{i+1}]$ .

There have been a few applications of the model with different rainfall data sets. These include modelling of (a) point rainfall data in Northern Greece (Koutsoyiannis and Foufoula-Georgiou, 1993); (b) areal rainfall in Italy (Mamassis et al., 1994) in a rainfall forecast framework; (c) intense rainfall at a point in Greece (Mamassis, 1997); (d) point rainfall in Florida, USA, in order to construct a continuous rainfall simulation model (Koutsoyiannis and Pachakis (1996); and (e) intense point rainfall based on intensity-duration-frequency curves at Athens, Greece, in an urban storm design framework (Koutsoyiannis and Zarris, 1999). Notably, in case (d) comparisons of simulated to historical data were made using not only typical statistical descriptors, but also descriptors used in chaos literature such as correlation dimensions and correlation integrals. The results showed a very satisfactory agreement between simulated and historical statistical descriptors.

### 3. The Bartlett-Lewis (BL) rectangular pulse point process

As mentioned above, the Bartlett-Lewis rectangular pulse model (Rodriguez-Iturbe et al., 1987, 1988; Onof and Wheater, 1993, 1994) is a stochastic model for the entire time domain (as opposed to the scaling model, which applies to rainy periods only). The model has been applied widely and there is much experience in calibrating it to several climates, which accumulated evidence on its ability to reproduce important features of the rainfall field from the hourly to the daily scale and above. The general assumptions of the Bartlett-Lewis rectangular pulse model are (see Figure 2): (1) storm origins  $t_i$  occur following a Poisson process with rate  $\lambda$ ; (2) origins  $t_{ij}$  of cells of each storm  $i$  arrive following a Poisson process with rate  $\beta$ ; (3) cell arrivals of each storm  $i$  terminate after a time  $V_i$  exponentially distributed with parameter  $\gamma$ ; (4) each cell has a duration  $W_{ij}$  exponentially distributed with parameter  $\eta$ ; and (5) each cell has a uniform intensity  $X_{ij}$  with a specified distribution.

In the original version of the model, all parameters are assumed constant. In the modified version, the parameter  $\eta$  is randomly varied from storm to storm with a gamma distribution



with shape parameter  $\alpha$  and scale parameter  $\nu$ . Subsequently, parameters  $\beta$  and  $\gamma$  also vary so that the ratios  $\kappa := \beta / \eta$  and  $\varphi := \gamma / \eta$  are constant.

The distribution of the uniform intensity  $X_{ij}$  of cells is typically assumed exponential with parameter  $1 / \mu_X$ , where  $\mu_X := E[X]$  (indices  $i$  and  $j$  are omitted due to stationarity). Alternatively, it can be chosen as two-parameter gamma with mean  $\mu_X$  and standard deviation  $\sigma_X$ . Thus, in its most simplified version the model uses five parameters, namely  $\lambda, \beta, \gamma, \eta$ , and  $\mu_X$  (or equivalently,  $\lambda, \kappa, \varphi, \eta$ , and  $\mu_X$ ) and in its most enriched version seven parameters, namely  $\lambda, \kappa, \varphi, \alpha, \nu, \mu_X$  and  $\sigma_X$ .

The equations of the BL model, in its original or the modified (random parameter) configuration, may be found in the appropriate references (Rodriguez-Iturbe et al., 1987, 1988; Onof and Wheater, 1993, 1994). These equations relate the statistical properties of the rainfall process in discrete time in the entire time domain, to the model parameters and serve as the basis for model fitting using these statistical properties. However, the focus of the present study is not on the entire time domain, but rather on the storm event only. Therefore, we need equations of the same statistical properties for the storm event. If we neglect the possibility of overlapping of storms (assuming that  $\lambda \ll \beta, \gamma, \eta$ ) then it is easy to derive such equations, as the process of interest in rainy periods becomes similar to the Poisson rectangular pulses model (Rodriguez-Iturbe et al., 1984). In Appendix A2 we have derived expressions for the rainfall intensity in continuous time in a storm. It may be seen that the process in a storm is not strictly stationary because of the boundary (origin) effect. If for simplification we neglect this effect, we find that the instant intensity  $\Xi(t | D)$  at time  $t$  in a storm of duration  $D$  has mean

$$E[\Xi(t | D)] = \kappa E[X] \quad (15)$$

and covariance

$$\text{Cov}[\Xi(t | D), \Xi(t + \tau | D)] = \kappa E[X^2] e^{-\eta \tau} \quad (16)$$

for the original BL model, and

$$\text{Cov}[\Xi(t | D), \Xi(t + \tau | D)] = \kappa E[X^2] \left( \frac{v + \varphi D}{v + \varphi D + \tau} \right)^{\alpha+1} \quad (17)$$

for the random parameter BL model.

It is easy then to derive similar expressions in discrete time (see Appendix A3). For both model versions the mean in discrete time with step  $\Delta$  is

$$E[Y_i] = \kappa E[X] \Delta \quad (18)$$

where  $Y_i$  is the incremental rainfall depth at time interval  $i$  of length  $\Delta$ . The second-order moments for the original model version are

$$\text{Var}[Y_i] = \frac{2 \kappa E[X^2]}{\eta^2} (\eta \Delta - 1 + e^{-\eta \Delta}) \quad (19)$$

$$\text{Cov}[Y_i, Y_{i+m}] = \frac{\kappa E[X^2]}{\eta^2} (1 - e^{-\eta \Delta})^2 e^{-\eta(m-1)\Delta} \quad (20)$$

$$\text{Corr}[Y_i, Y_{i+m}] = (1 - e^{-\eta \Delta})^2 e^{-\eta(m-1)\Delta} / 2 (\eta \Delta - 1 + e^{-\eta \Delta}) \quad (21)$$

where  $m > 1$ . The corresponding equations for the random parameter model version are

$$\text{Var}[Y_i] = \frac{2 \kappa E[X^2] (v + \varphi D)^2}{\alpha (\alpha - 1)} (\theta_1^{\alpha-1} + \frac{\alpha-1}{\theta_1} - \alpha) \quad (22)$$

$$\text{Cov}[Y_i, Y_{i+m}] = \frac{2 \kappa E[X^2] (v + \varphi D)^2}{\alpha (\alpha - 1)} \left[ (1/2) (\theta_{m+1}^{\alpha-1} + \theta_{m-1}^{\alpha-1}) - \theta_m^{\alpha-1} \right] \quad (23)$$

$$\text{Corr}[Y_i, Y_{i+m}] = \left[ (1/2) (\theta_{m+1}^{\alpha-1} + \theta_{m-1}^{\alpha-1}) - \theta_m^{\alpha-1} \right] / (\theta_1^{\alpha-1} + \frac{\alpha-1}{\theta_1} - \alpha) \quad (24)$$

where

$$\theta_m = \frac{v + \varphi D}{v + \varphi D + m \Delta} \quad (25)$$

The mean and variance of the total storm depth can be determined from (18) and (19) (or (22) for the random parameter model version), respectively, setting  $\Delta = D$ . The above equations may serve as a basis for parameter estimation using information from the rainy periods only.

We can notice in the above equations that (under the assumptions made) the statistics of the rainfall process within a storm depend on the parameters  $\kappa$  and  $\eta$  (or the parameters of the latter's distribution), and the parameters of the distribution of  $X_{ij}$  (namely,  $E[X]$ ,  $E[X^2]$ ). In the random parameter model version they are also affected by the parameter  $\varphi$  whereas in neither version is affected by the parameters  $\lambda$ . In fact, the three parameters  $\kappa$ ,  $E[X]$  and  $E[X^2]$  are combined in two, namely  $\kappa E[X]$ ,  $\kappa E[X^2]$ . Therefore, it is no loss of generality to assume that  $X_{ij}$  is exponentially distributed, in which case  $E[X^2] = 2 E^2[X]$ , so that we have two independent parameters, namely  $\kappa$  and  $\mu_X \equiv E[X]$ . In addition, we have the parameter  $\eta$  for the original model version and parameters  $\alpha$ ,  $\nu$  and  $\varphi$  for the random parameter model version.

Contrary to the scaling model, the mean  $E[Y_i]$  and the standard deviation  $\text{Std}[Y_i]$  of the incremental depths do not depend on duration  $D$  and are constant for all storms in the original model version. Also constant, independent of duration, is the autocorrelation coefficient of any lag for this version. In the random parameter version the standard deviation and the autocorrelation coefficient depend on duration  $D$  but the mean is still constant. Another difference among the two model versions is that the decay of the autocorrelation function is milder in the random parameter model version.

#### 4. Data sets

Two data sets were used for the exploration and comparison of models. The first data set is point rainfall at the Zographou meteorological station, Athens, Greece (latitude  $37^{\circ}58'26''\text{N}$ , longitude  $23^{\circ}47'16''\text{E}$ , altitude 219 m), for 6 years (1993-99). The available time resolution of measurements is ten minutes and the depth resolution is 0.1 mm. The mean annual rainfall in the area is around 450 mm. The separation time to identify different events was assumed to be 6 h. Only intense storms were chosen from the available record, i.e., those with hourly depth exceeding 5 mm or daily depth exceeding 15 mm. Thus, a total of 81 storms were extracted, which were classified in five classes (marked as 1 to 5) according to their durations, as shown in Table 1. The available temporal resolution  $\Delta = 10$  min was used to assemble Table 1. The basis for selecting these classes was to have approximately the same number of storms within each class. For each class a mean duration  $E[D]$  was estimated from data, equal

to the mean of durations of all storms in this class, and assigned as the representative duration for the class. Standard deviations of storm durations, as well as means and standard deviations of the total and incremental depths, and lag-one autocorrelation coefficients of incremental depths were also estimated from data for each class and are also shown in Table 1. The storms were further grouped into two larger classes (A and B, also shown in Table 1), which were necessary to achieve reliable estimates of autocorrelation coefficients for larger lags. In addition, to assess the effect of the temporal resolution, the set of storms was processed using a larger temporal resolution,  $\Delta = 1$  h, and the resulting characteristics of the classes are tabulated in Table 2 in a similar manner as in Table 1.

The second data set is point rainfall at the Parrish raingauge Florida, USA (altitude 40 m), for 19 years (1971-89). The available time resolution of measurements is 15 minutes and the depth resolution is 0.1 in  $\approx$  3 mm. The mean annual rainfall in the area is 1290 mm. The separation time to identify different events was assumed to be 6 h. All storms (1643 in total) of the 19-year period were assembled from the available record. The 1643 storms were classified in 10 classes (marked as 1 to 10) according to their durations, as shown in Table 3 for temporal resolution  $\Delta = 15$  min and in Table 4 for a larger temporal resolution,  $\Delta = 2$  h. Here we intentionally chose the 2 h (rather than the ‘standard’ 1 h) resolution to assess the performance of models in describing rainfall events at a temporal resolution as coarser as possible. This is almost one order of magnitude coarser than the original of 15 min; an even coarser resolution would obscure the event structure too much (the mean storm duration is 2.28 h). As in the Zographou data set, a second grouping using two classes (A and B) was made, which is also shown in Table 3 and Table 4.

The standard deviations of the total depths ( $\text{Std}[H] =: \sigma_H$ ) shown in Table 1 through Table 4 are corrected according to

$$\sigma_H^2 = \frac{\sigma_H'^2 - \mu_H^2 (1 + \kappa)^2 \sigma_D^2 / \mu_D^2}{1 + (1 + \kappa)^2 \sigma_D^2 / \mu_D^2} \quad (26)$$

where  $\sigma_H$  and  $\sigma'_H$  are the corrected and the raw estimate of standard deviation of the total depth of each class, respectively,  $\mu_H$  is the average total depth of the same class,  $\mu_D$  and  $\sigma_D$  are the mean and standard deviation of the duration of each class, and  $\kappa$  is the scaling exponent of (1) estimated from (12). This correction was necessary because the raw estimate of variance using the data values of  $H$  of each class is affected by the variability of duration in each class (expressed by  $\sigma_D^2$ ), which in some cases (the classes with the larger durations) is very significant. The justification of (26) is given in Appendix A4, where it is also shown that an analogous correction for the mean of  $H$  is not necessary.

Another correction may be needed for the mean of  $D$  in the class with the lowest durations (class 1). This problem is apparent in class 1 of Table 3, where all 608 events seemingly have duration equal to 0.25 h. However, this is due to the available temporal resolution of  $\Delta = 0.25$  h. All storms with durations smaller than  $\Delta = 0.25$  h are erroneously assigned a duration of 0.25 h. Therefore, the actual mean of class 1 of Table 3 must be less than 0.25 h. Assuming that durations are exponentially distributed, it can be shown that the correct mean duration of this class is about 0.05 h. However, we preferred not to apply this correction and exclude this class from further processing.

## 5. Comparisons and further developments

The scaling model of storm hyetograph was fitted to both Zographou and Parrish data sets, using the finest available temporal resolution (10 and 15 min, respectively) and the methodology already described in section 2. The estimated parameters are shown in Table 5. In a similar manner the parameters of the BL model were estimated for both data sets. Specifically, the product  $\kappa \mu_X$ , which has a common value for both model versions, was estimated from (18) as the average of  $E[Y]$  of all classes divided by  $\Delta$ . Then the product  $\kappa E[X^2]$  and the parameter  $\eta$  of the original version or the parameters  $\alpha$ ,  $\nu$  and  $\varphi$  of the random parameter version were estimated simultaneously by minimising the fitting error of the model in  $\text{Var}[H]$ ,  $\text{Var}[Y]$  and  $\text{Corr}[Y_i, Y_{i+1}]$  for all classes. Parameters  $\kappa$  and  $\mu_X$  were then determined from the known products  $\kappa \mu_X$  and  $\kappa E[X^2]$  assuming an exponential distribution for  $X$ , i.e.,

$E[X^2] = 2 \mu_X^2$ . The estimated parameters are shown in Table 6 for the original BL model version and in Table 7 for the random parameter BL model version.

Now we are able to intercompare the scaling model and the BL model based on their agreement with the historical storm data. This is done graphically in Figure 3 through Figure 9. Each of these figures contains a sequence of points corresponding to the historical data and four curves corresponding to the scaling model, the two versions of the BL model, and one additional version of the latter which will be discussed later in this section. Furthermore, each of these figures includes four cases, of which cases (a) and (c) refer to the Zographou and Parrish data sets, respectively, for the finer available temporal resolutions ( $\Delta = 10$  and 15 min, respectively). Similar are cases (b) and (d) but they refer to the coarser temporal resolutions ( $\Delta = 1$  and 2 h for Zographou and Parrish, respectively). We emphasise that the model parameters were not fitted separately for the coarser temporal resolutions, but rather those estimated from the finest resolutions were used in cases (b) and (d), too. In this way we can test whether a parameter set estimated from one resolution is appropriate for another resolution, too.

Figure 3 refers to the mean of total storm depth as a function of storm duration (logarithmic plot). To plot the empirical means, the mean duration of each duration class was used. One theoretical curve is plotted for both versions of the BL model, which was determined by (18) for  $\Delta = D$ . This is a straight line with slope equal to one for all cases. On the other hand, the scaling model yields another straight line with slope equal to 0.46 in the Zographou case and 0.40 in the Parrish case. Clearly, the scaling model outperforms the BL model in all cases. The latter exhibits large departures from data, the most significant being the one for Parrish with  $\Delta = 2$  h (Figure 3(d)). This indicates the inappropriateness of a specific parameter set for a temporal resolution different from the one that was used for the model fitting. A more careful observation reveals that the appearing discrepancies are not due to inappropriate parameters but rather are related to the model structure, which implies a straight line with slope equal to one, regardless of the parameter values.

Figure 4 depicts the models' behaviour regarding the standard deviation of total storm depth as a function of storm duration. Here all models performed equally well for Zographou,

but there are some slight departures of the BL model for Parrish, especially in the case with  $\Delta = 2$  h (Figure 4(d)).

Figure 5 refers to the mean of incremental storm depth. As in Figure 3, one theoretical curve is plotted for both versions of the BL model, which again was determined by (18) for the appropriate time interval  $\Delta$  of each case. According to the BL model, the mean of incremental depth is constant, independent of the duration  $D$ . However, the data show a clear decreasing trend of the mean incremental depth with the increase of storm duration. This trend is very well captured by the scaling model in all cases. Thus, the scaling model outperforms the BL model, especially in case of Figure 5(d) (Parrish,  $\Delta = 2$  h) where the BL model predicts values far higher than the actual ones. Again the problem here is due to the model structure rather than the parameter values.

Figure 6 shows the empirical and theoretical standard deviation of incremental storm depth as a function of storm duration. Again here the empirical data indicate a decreasing trend of the standard deviation of incremental depth with the increase of storm duration. The scaling model captures this trend in all cases, whereas the BL model suggests a constant standard deviation of the incremental storm depth, independent of storm duration, or even an opposite (increasing) trend in the case of the random parameter model version (more apparent in Figure 6 (b)).

Figure 7 depicts the variation of the lag-one autocorrelation coefficient of incremental storm depth with storm duration. Empirical data suggest an increasing trend of the autocorrelation coefficient with duration, which is captured well by the scaling model and much less by the random parameter model version, whereas the original BL model implies that this coefficient should be constant. The departures of BL model from data is not very significant in this case.

Figure 8 and Figure 9 depict the empirical and theoretical autocorrelation functions for lags up to 10 of incremental storm depth for small and large storm durations, respectively (classes A and B, respectively). In the case of small durations (Figure 8) all models perform almost equally well. However, Figure 9, in comparison with Figure 8, suggests that empirical autocorrelation functions tend to decay more slowly for large durations than for small ones.

This again is captured by the scaling model, whereas in both BL model versions the theoretical curves are identical in both Figure 8 and Figure 9.

Additional comparisons were made to assess the effect of seasonality to model parameters. Thus, the entire analysis for the Parrish data set was repeated using two seasons: from June to September (790 mm total depth; rainy season) and from October to May (dry season). Plots similar with those of Figure 3 through Figure 9 were constructed using the single parameter set estimated from data of the whole year. These plots, which have not been included in the paper, indicated that the single parameter set was almost equally good for both seasons.

The entire analysis indicates a better performance of the scaling model in comparison with the BL model in terms of capturing the empirical characteristics of storms. The worse performance of the BL model is mainly due to the fact that it does not capture the empirical relationship of the means of total and incremental storm depths with duration (Figure 3 and Figure 5). On the contrary, the fit of the scaling model is perfect in this case, owing to the scaling exponent  $\kappa$  whose value is  $-0.54$  for Zographou and  $-0.60$  for Parrish (Table 5). Had this value been closer to zero (as indeed was in most of the case studies mentioned in section 2), the departure of the BL model (which in fact assumes  $\kappa = 0$ ) would be lower.

The examined model BL versions, i.e., the original and random parameter versions, both imply a common expression of the mean incremental depth, i.e.,  $E[Y_i] = \kappa E[X] \Delta$  (equation (18)). We note that the random parameter version varies randomly the parameter  $\eta$ , and consequently  $\beta$ , so that both the mean cell duration  $1 / \eta$  and the mean interarrival time of cells  $1 / \beta$  become increasing functions of the storm durations. Specifically, these functions can be expressed by

$$E[1 / \eta | D] = \frac{v + \varphi D}{\alpha}, \quad E[1 / \beta | D] = \frac{v + \varphi D}{\kappa \alpha} \quad (27)$$

as it follows from the results of Appendix A2 (equation (A.32)). This means that in a storm of a large duration, cells tend to last longer on average (higher  $1 / \eta$ ), and at the same time are more spaced out (higher  $1 / \beta$ ). These two tendencies are mutually counterbalanced, as far as average rainfall intensity is concerned, because the two relations in (27) are proportional to



each other. In other words, this is the consequence of the assumption of a constant  $\kappa$ , which must be considered as the main reason why both BL model versions have practically the same performance in this study.

Thus, the question arises whether a modified version of the Bartlett-Lewis model would be in better agreement with the empirical data. To assess this, we attempted to introduce dependence of the parameter  $\kappa$  on duration, described by a power relationship, i.e.,

$$\kappa = \kappa_0 D^{\kappa_1} \quad (28)$$

We assume a similar relationship for  $\eta$ , i.e.,

$$\eta = \eta_0 D^{\eta_1} \quad (29)$$

in which case the parameter  $\beta$  varies accordingly as

$$\beta = \beta_0 D^{\beta_1} \quad (30)$$

where  $\beta_0 = \kappa_0 \eta_0$  and  $\beta_1 = \kappa_1 + \eta_1$ . We expect that both exponents  $\kappa_1$  and  $\eta_1$  (and consequently  $\beta_1$ , too) are smaller than zero. In this manner, the mean cell duration  $1 / \eta$  and the mean interarrival time of cells  $1 / \beta$  will be increasing functions of the storm durations, which agrees with the remark of Rodriguez-Iturbe et al. (1988) that storms made up of cells with longer durations tend to last longer and to have longer interarrival times between cells.

In the testing framework of this paper it is easy to implement this adaptation of the BL model, because the storm duration  $D$  is known. All equations of the original model version are still valid, if we simply substitute  $\kappa$  and  $\eta$  with their expressions from (28) and (29), respectively. In the parameter sets obtained in this case, five parameters can be estimated from the data, namely  $\mu_X$ ,  $\kappa_0$ ,  $\kappa_1$ ,  $\eta_0$  and  $\eta_1$ , while the two additional parameters  $\lambda$  and  $\gamma$  are beyond the scope of this work. The parameter  $\kappa_1$  was set equal to  $\kappa$  of the scaling model and all other parameters were estimated in the manner described above. All fitted parameters of this model version are given in Table 8. The resulting modelled characteristics of total and incremental depths are depicted in Figure 3 through Figure 9, marked as ‘BL/additional’ among with the curves of the other model, which were described above. We observe that in

Figure 3 and Figure 5, where the two known versions of the BL model had the worst performance, the additional BL version becomes identical to the scaling model and, thus, it agrees very well with empirical data. In all other figures the additional BL model version outperforms the known two versions and fits the empirical data equally well with (in some instances slightly better than) the scaling model.

## 6. Conclusions and discussion

An intercomparison of two stochastic models of the rainfall process, belonging to different categories, has been attempted in this paper. The first is the scaling model of storm hyetograph, which belongs to the category of storm-based models. The second is the Bartlett-Lewis rectangular pulse model, the most widespread among the category of point process models. The scaling model is further developed introducing one more parameter to better fit historical data. The Bartlett-Lewis model is theoretically studied to extract mathematical relationships for the intra-storm structure. The intercomparison is based on the storm hyetographs of a data set from Greece and another one from the USA. The different storms are identified in each data set and classified according to their duration. A systematic study of the structure of storm hyetographs is used to assess how well certain characteristics of the hyetographs can be reproduced by the two stochastic models. Both models are fitted using the characteristics of storms. The comparison shows that the scaling model of storm hyetograph agrees well with the structure of historical hyetographs whereas the Bartlett-Lewis rectangular pulse model exhibits some discrepancies in either its original version or its random parameter version. However, it is shown that the performance of the Bartlett-Lewis model is significantly improved, and becomes comparable to that of the scaling model, by introducing a power-law dependence of its cell related parameters (duration and rate of arrivals) on the storm duration.

It must be emphasised that the fitting of the Bartlett-Lewis model used in this paper serves the purposes of this intercomparison study only and it is not appropriate for an operational modelling application. Specifically, the fitting procedure used refers to a part of the model's parameter set and it is not free of simplifying assumptions (e.g. ignorance of storm

overlapping) and subjectivities (e.g., choice of storm classes). Despite of the assumptions and subjectivities, the testing framework is able to locate structural weak points of the Bartlett-Lewis model, which may be responsible for the known difficulties to describe the statistical structure of rainfall at a wide range of scales (particularly at the sub-storm timescales) using the same parameter values.

The proposed adaptation of the Bartlett-Lewis model by introducing a power-law dependence of its cell related parameters on the storm duration, which is a sort of merging of the Bartlett-Lewis point process model to the scaling model, seems to be a promising improvement. Further research is required, however, to implement this adaptation into an operational model to be used for simulation. Specifically, the power laws may be expressed in terms of the Bartlett-Lewis model ‘storm’ duration  $V$  rather than the measurable duration of each storm event  $D$  that was used in this study. In addition, expressions for the statistics of the incremental depth over the entire time domain are needed, in addition to those derived in this study that are focused on the interior of a storm. Such expressions will make feasible a more robust parameter technique for the adapted model.

**Acknowledgments.** We thank Christian Onof and an anonymous reviewer for their detailed, positive and constructive reviews which resulted in significant improvements of the paper.

## References

- Bo, Z., and S. Islam (1994). Aggregation-disaggregation properties of a stochastic rainfall model, *Water Resour. Res.*, 30(12), 3423-3435.
- Cameron, D., K. Beven, and J. Tawn (2000). An evaluation of three stochastic rainfall models, *Journal of Hydrology*, 228 (1-2), 130-149.
- Copertwait, P. S. P. (1991). Further developments of the Neyman-Scott clustered point process for modeling rainfall, *Water Resour. Res.*, 27(7), 1431-1438.
- Copertwait, P. S. P. (1998). A Poisson-cluster model of rainfall: high-order moments and extreme values, *Proc. R. Soc. Lond. A*, 454, 885-898.
- Cowpertwait, P. S. P., P. E. O'Connell, A. V. Metcalfe, and J. A. Mawdsley (1996a). Stochastic point process modelling of rainfall, I, Single-site fitting and validation, *J. of Hydrol.*, 175 (1-4), 17-46.
- Cowpertwait, P. S. P., P. E. O'Connell, A. V. Metcalfe, and J. A. Mawdsley (1996b). Stochastic point process modelling of rainfall, II, Regionalisation and disaggregation, *J. of Hydrol.*, 175 (1-4), 47-65.
- Eagleson, P. S. (1970). *Dynamic Hydrology*, McGraw-Hill.
- Eagleson P. S. (1978). Climate, soil and vegetation, 2, The distribution of annual precipitation derived from observed storm sequences, *Water Resources Research*, 14(5), 713-721.
- Foufoula-Georgiou, E., P. and Guttorp (1986). Compatibility of continuous rainfall occurrence models with discrete rainfall observations, *Water Resources Research*, 22(8), 1316-1322.
- Foufoula-Georgiou, E, and W. Krajewski (1995). Recent advances in rainfall modeling, estimation, and forecasting, *Reviews of Geophysics*, 33, (1125-1137).
- Foufoula-Georgiou, E. and D. P. Lettenmaier (1986). Continuous-time versus discrete-time point process models for rainfall occurrence series, *Water Resources Research*, 22(4), 531-542.
- Glasbey, C.A., G. Cooper, and M. B. McGehan (1995). Disaggregation of daily rainfall by conditional simulation from a point-process model, *J. of Hydrol.*, 165, 1-9.

- Grace, R. A. and P. S. Eagleson (1966). The synthesis of short-time-increment rainfall sequences, Report no. 91, Hydrodynamics Laboratory, Massachusetts Institute of Technology, Cambridge, Mass.
- Guttorp, P. (1986). On binary time series obtained from continuous point processes describing rainfall, *Water Resources Research*, 22(6), 897-904.
- Gyasi-Agyei, Y. (1999). Identification of regional parameters of a stochastic model for rainfall disaggregation, *Journal of Hydrology*, 223(3-4), 148-163.
- Gyasi-Agyei, Y., and G. R. Willgoose (1997). A hybrid model for point rainfall modeling, *Water Resour. Res.*, 33(7), 1699-1706.
- Gyasi-Agyei, Y., and G. R. Willgoose (1999). Generalisation of a hybrid model for point rainfall, *Journal of Hydrology*, 219 (3-4), 218-224.
- Huff, F. A. (1967). Time distribution of rainfall in heavy storms, *Water Resources Research*, 3(4), 1007-1019.
- Kakou, A. (1997). Point process based models for rainfall, PhD thesis, University College London, London.
- Khaliq, M. N., and C. Cunnane (1996). Modelling point rainfall occurrences with the Modified Bartlett-Lewis Rectangular Pulses Model, *J. of Hydrol.* 180(1-4), 109-138.
- Koutsoyiannis, D. (1988). A point rainfall disaggregation model, PhD thesis (in Greek), National Technical University, Athens.
- Koutsoyiannis, D. (1994). A stochastic disaggregation method for design storm and flood synthesis, *Journal of Hydrology*, 156, 193-225.
- Koutsoyiannis, D., and E. Foufoula-Georgiou (1993). A scaling model of storm hyetograph, *Water Resources Research*, 29(7), 2345-2361.
- Koutsoyiannis, D., and C. Onof (2001). Rainfall disaggregation using adjusting procedures on a Poisson cluster model, *Journal of Hydrology*, 2001 (in press).
- Koutsoyiannis, D., and D. Pachakis (1996). Deterministic chaos versus stochasticity in analysis and modeling of point rainfall series, *Journal of Geophysical Research – Atmospheres*, 101(D21), 26 444-26 451.

- Koutsoyiannis, D., and Th. Xanthopoulos (1990). A dynamic model for short-scale rainfall disaggregation, *Hydrological Sciences Journal*, 35(3), 303-322.
- Koutsoyiannis, D., and D. Zarris (1999). Simulation of rainfall events for design purposes with inadequate data, XXIV General Assembly of European Geophysical Society, The Hague, *Geophys. Res. Abstracts*, vol. 1, p. 296.
- Mamassis, N., (1997). Rainfall analysis by weather type, PhD thesis (in Greek), National Technical University, Athens.
- Mamassis, N., D. Koutsoyiannis, and E. Foufoula-Georgiou (1994). Stochastic rainfall forecasting by conditional simulation using a scaling storm model, XIX General Assembly of European Geophysical Society, Grenoble, *Annales Geophysicae*, Vol. 12, Suppl. II, Part II, pp. 324, 408.
- Marien, J. L. and G. L. Vandewiele (1986). A point rainfall generator with internal storm structure, *Water Resour. Res.*, 22(4), 475-482.
- Onof, C., H. S. Wheater and V. Isham (1994). Note on the analytical expression of the inter-event time characteristics for Bartlett-Lewis type rainfall models, *J. of Hydrol.*, 157, 197-210.
- Onof, C. and H. S. Wheater (1993). Modelling of British rainfall using a Random Parameter Bartlett-Lewis Rectangular Pulse Model, *J. Hydrol.*, 149, 67-95.
- Onof, C. and H. S. Wheater (1994). Improvements to the modeling of British rainfall using a Modified Random Parameter Bartlett-Lewis Rectangular Pulses Model, *J. Hydrol.*, 157, 177-195.
- Restrepo-Posada, P. J. and P. S. Eagleson, (1982). Identification of independent rainstorms, *Journal of Hydrology*, 55, 303-319.
- Rodriguez-Iturbe, D. R. Cox, and V. Isham (1987). Some models for rainfall based on stochastic point processes, *Proc. R. Soc. Lond.*, A 410, 269-298.
- Rodriguez-Iturbe, D. R. Cox, and V. Isham (1988). A point process model for rainfall: Further developments, *Proc. R. Soc. Lond.*, A 417, 283-298.
- Rodriguez-Iturbe, I., V. K. Gupta, and E. Waymire (1984). Scale considerations in the modeling of temporal rainfall, *Water Resources Research*, (20(11), 1611-1619.

- Smith, J. A. and A. F. Karr, (1983). A point process model of summer season rainfall occurrences, *Water Resources Research*, 19(1), 95-103.
- Valdes, J. B., I. Rodriguez-Iturbe, and V. K. Gupta (1985). Approximations of temporal rainfall from a multidimensional model, *Water Resources Research*, 21(8), 1259-1270.
- Velghe, T., P. A. Troch, F. P. De Troch, J. Van de Velde (1994). Evaluation of cluster-based rectangular pulses point process models for rainfall, *Water Resources Research*, 30(10), 2847-2857.
- Verhoest, N., P. A. Troch, and F. P. De Troch (1997). On the applicability of Bartlett-Lewis rectangular pulses models in the modeling of design storms at a point, *Journal of Hydrology*, 202, 108-120.
- Waymire, E. and V. K. Gupta, (1981a). The mathematical structure of rainfall representations, 2, A review of the theory of point processes, *Water Resources Research*, 17(5), 1273-1285.
- Waymire, E. and V. K. Gupta, (1981b). The mathematical structure of rainfall representations, 3, Some applications of the point process theory to rainfall processes, *Water Resources Research*, 17(5), 1287-1294.
- Woolhiser, D. A. and H. B. Osborn (1985). A stochastic model of dimensionless thunderstorm rainfall, *Water Resources Research*, 21(4) 511-522.

## Appendix: Derivation of equations

### A1. Expressions of variances and covariances in discrete time for the modified version of the scaling model

The expected value of the product  $Y_i Y_{i+m}$  is

$$E[Y_i Y_{i+m}] = E[Y_1 Y_{1+m}] = \int_0^{\Delta} \int_{m\Delta}^{(m+1)\Delta} E[\Xi(t_1) \Xi(t_2)] dt_1 dt_2 = \int_0^{\Delta} \int_{m\Delta}^{(m+1)\Delta} R_{\Xi}(t_2 - t_1) dt_1 dt_2 \quad (\text{A.1})$$

The double integral can be simplified by transforming its integration area, that is,

$$E[Y_i Y_{i+m}] = \int_{(m-1)\Delta}^{m\Delta} R_{\Xi}(\tau) [\tau - (m-1)\Delta] d\tau + \int_{m\Delta}^{(m+1)\Delta} R_{\Xi}(\tau) [(m+1)\Delta - \tau] d\tau \quad (\text{A.2})$$

A translation of the integration variable results in

$$E[Y_i Y_{i+m}] = \int_{-\Delta}^{\Delta} R_{\Xi}(m\Delta + \tau) (\Delta - |\tau|) d\tau \quad (\text{A.3})$$

Substituting  $R_{\Xi}(\tau)$  from (3) and also using (4) we get

$$E[Y_i Y_{i+m}] = \alpha D^{2\kappa} \int_{-\Delta}^{\Delta} \left[ \left| \frac{m\Delta + \tau}{D} \right|^{-\beta} - \zeta \right] (\Delta - |\tau|) d\tau \quad (\text{A.4})$$

which setting  $\Delta = \delta D$  and  $\tau = \chi \Delta = \chi \delta D$  becomes

$$E[Y_i Y_{i+m}] = \alpha \delta^2 D^{2(1+\kappa)} \int_{-1}^1 [\delta^{-\beta} |m + \chi|^{-\beta} - \zeta] (1 - |\chi|) d\chi \quad (\text{A.5})$$

After algebraic manipulations this becomes (for  $m \geq 1$ )

$$E[Y_i Y_{i+k}] = \alpha \delta^2 D^{2(1+\kappa)} \frac{\{(1/2)[(m-1)^{2-\beta} + (m+1)^{2-\beta}] - m^{2-\beta}\} \delta^{-\beta} - \zeta(\beta-1)(\beta-1/2)}{(\beta-1)(\beta-1/2)} \quad (\text{A.6})$$

which by virtue of (9), (10) and (11) writes



$$E[Y_i Y_{i+k}] = D^{2(1+\kappa)} \delta^2 \frac{(c_1^2 + c_2)[\delta^{-\beta} f(m, \beta) - \varepsilon]}{1 - \varepsilon} \quad (\text{A.7})$$

Then using (5), the derivation of (7) is straightforward.

For  $m = 0$ , (A.5) writes (due to symmetry)

$$E[Y_i^2] = 2 \alpha \delta^2 D^{2(1+\kappa)} \int_0^1 (\delta^{-\beta} \chi^{-\beta} - \zeta) (1 - \chi) d\chi \quad (\text{A.8})$$

or

$$E[Y_i^2] = 2 \alpha \delta^2 D^{2(1+\kappa)} \frac{\delta^{-\beta} - \zeta(\beta - 1)(\beta - 1/2)}{(\beta - 1)(\beta - 1/2)} \quad (\text{A.9})$$

which again can be written in the form of (A.7) with  $f(0, \beta) = 1$  (by virtue of (10)). The derivation of (6) is then straightforward. Furthermore, (13) is a direct consequence of (6) obtained for  $\delta = 1$ .

## **A2. Expressions for the rainfall intensity in continuous time in a storm for the rectangular pulse Bartlett-Lewis model**

We assume that the rate of storm arrivals  $\lambda$  is much less than the rate of cell arrivals  $\beta$  within a storm ( $\lambda \ll \beta$ ) so that we can ignore the possibility of storm overlapping. The duration  $W$  of each cell is exponentially distributed with parameter  $\eta$  ( $F_W(w) = 1 - \exp(-\eta w)$ ) and its intensity  $X$  is uniform through duration  $W$  with a specified distribution  $F_X(x)$ .

The rainfall intensity  $\Xi(t)$  at time  $t$  is the sum of the contributions of several cells  $X_j$  that arrived some time  $t_j$  before  $t$  and lasted more than  $t - t_j$ . We divide the time before  $t$  into small intervals  $I_i$  of length  $\Delta a$  setting  $a_0 \equiv t$ ,  $a_1 = t - \Delta a$ ,  $a_2 = t - 2\Delta a$ , ..., and  $I_i := (a_i, a_{i-1}]$ . We denote by  $\Delta n_i$  the number of cell arrivals within each  $I_i$ . The probability that  $\Delta n_i = 1$  is  $\beta \Delta a$  whereas the probability that  $\Delta n_i = 0$  is  $1 - \beta \Delta a$  (we can neglect the probability  $\Delta n_i > 1$  because  $\Delta a$  is small). We also denote by  $X_i$  the intensity of the rain cell arrived at the interval  $I_i$  and  $\Delta \Xi(t, a_i)$  the rainfall intensity at time  $t$  due to that cell. Thus,

$$\Xi(t) = \sum_i \Delta \Xi(t, a_i) \quad (\text{A.10})$$

Now, if  $\Delta n_i = 0$  then obviously  $\Delta \Xi(t, a_i) = 0$  whereas if  $\Delta n_i = 1$  then

$$\Delta \Xi(t, a_i) = \begin{cases} X_i & \text{if } W_i > a_i \\ 0 & \text{if } W_i < a_i \end{cases} \quad (\text{A.11})$$

Consequently,

$$E[\Delta \Xi(t, a_i) | \Delta n_i = 1] = E[X_i] P(W_i > a_i) \quad (\text{A.12})$$

where  $P(\ )$  denotes probability, or,

$$E[\Delta \Xi(t, a_i) | \Delta n_i = 1] = E[X] [1 - F_W(a_i)] \quad (\text{A.13})$$

and

$$E[\Delta \Xi(t, a_i)] = E[\Delta \Xi(t, a_i) | \Delta n_i = 1] P(\Delta n_i = 1) \quad (\text{A.14})$$

or

$$E[\Delta \Xi(t, a_i)] = E[X] [1 - F_W(a_i)] \beta \Delta a \quad (\text{A.15})$$

Taking expected values in (A.10), combining (A.15) and also assuming  $\Delta a \rightarrow 0$ , we get

$$E[\Xi(t)] = \int_0^t E[X] [1 - F_W(a)] \beta da + E[X] [1 - F_W(t)] \quad (\text{A.16})$$

where we have assumed that the storm have started at time  $t = 0$ . The last term in the right-hand side of (A.16) is the contribution of the first cell of the storm, which in the Bartlett-Lewis model is assumed to arrive at  $t = 0$ . Substituting the exponential expression of  $F_W(a)$  in (A.16) we get

$$E[\Xi(t)] = \beta E[X] \int_0^t \exp(-\eta a) da + E[X] \exp(-\eta t) \quad (\text{A.17})$$

and after algebraic manipulations

$$E[\Xi(t)] = \kappa E[X] + (1 - \kappa) E[X] \exp(-\eta t) \quad (\text{A.18})$$

where we have substituted  $\beta / \eta = \kappa$ . The second term in the right-hand side of (A.18) represents the boundary effect. For large  $t$  (A.18) simplifies to (15).

Furthermore, we consider the product

$$\Xi(t) \Xi(t + \tau) = \sum_i \Delta\Xi(t, a_i) \sum_j \Delta\Xi(t + \tau, a_j) \quad (\text{A.19})$$

for  $\tau > 0$ . When  $a_i \neq a_j$ ,  $\Delta\Xi(t, a_i)$  is independent to  $\Delta\Xi(t + \tau, a_j)$ , because they correspond to different rain cells, and therefore

$$E[\Delta\Xi(t, a_i) \Delta\Xi(t + \tau, a_j)] = E[\Delta\Xi(t, a_i)] E[\Delta\Xi(t + \tau, a_j)] \quad (\text{A.20})$$

When  $a_i = a_j$ ,  $\Delta\Xi(t, a_i)$  and  $\Delta\Xi(t + \tau, a_j)$  correspond to the same cell. Therefore, if  $\Delta n_i = 1$  then

$$\Delta\Xi(t, a_i) \Delta\Xi(t + \tau, a_i) = \begin{cases} X_i^2 & \text{if } W_i > a_i + \tau \\ 0 & \text{if } W_i < a_i + \tau \end{cases} \quad (\text{A.21})$$

whereas if  $\Delta n_i = 0$  then obviously  $\Delta\Xi(t, a_i) \Delta\Xi(t + \tau, a_i) = 0$ . Consequently,

$$E[\Delta\Xi(t, a_i) \Delta\Xi(t + \tau, a_i) \mid \Delta n_i = 1] = E[X_i^2][1 - F_W(a_i + \tau)] \quad (\text{A.22})$$

and

$$E[\Delta\Xi(t, a_i) \Delta\Xi(t + \tau, a_i)] = E[X_i^2][1 - F_W(a_i + \tau)] \beta \Delta a \quad (\text{A.23})$$

Taking expected values in (A.19), combining (A.20) and (A.23) and also assuming  $\Delta a \rightarrow 0$ , we get

$$\begin{aligned} E[\Xi(t) \Xi(t + \tau)] &= \int_0^t E[X_i^2][1 - F_W(a + \tau)] \beta da + E[X_i^2][1 - F_W(t + \tau)] \\ &\quad + E[\Xi(t)] E[\Xi(t + \tau)] \end{aligned} \quad (\text{A.24})$$

and

$$\text{Cov}[\Xi(t), \Xi(t + \tau)] = \int_0^t E[X_i^2] [1 - F_W(a + \tau)] \beta da + E[X_i^2] [1 - F_W(t + \tau)] \quad (\text{A.25})$$

Again we have assumed that the storm have started at time  $t = 0$  and the last term in the right-hand side of (A.25) is the contribution of the first cell of the storm. Substituting the expression of  $F_W(a)$  in (A.25) we get

$$\text{Cov}[\Xi(t), \Xi(t + \tau)] = \beta E[X_i^2] \int_0^t \exp[-\eta (a + \tau)] da + E[X_i^2] \exp[-\eta (t + \tau)] \quad (\text{A.26})$$

and after algebraic manipulations

$$\text{Cov}[\Xi(t), \Xi(t + \tau)] = \kappa E[X_i^2] \exp(-\eta \tau) + (1 - \kappa) E[X_i^2] \exp[-\eta (t + \tau)] \quad (\text{A.27})$$

where we have substituted  $\beta / \eta = \kappa$ . The second term in the right-hand side of (A.27) represents the boundary effect. For large  $t$  (A.27) simplifies to (16).

In the case of the modified Bartlett-Lewis rectangular pulse model (A.18) represents the conditional mean for given  $\eta$ . The probability density function of  $\eta$  is

$$f_H(\eta) = \frac{v^\alpha \eta^{\alpha-1} e^{-v \eta}}{\Gamma(\alpha)} \quad (\text{A.28})$$

We assume that the distribution function of the storm duration  $D$  is practically equal to that of  $V$  (see section 3 and Figure 2), that is

$$f_{D|H}(d | \eta) = \gamma e^{-\gamma d} = \varphi \eta e^{-\varphi \eta d} \quad (\text{A.29})$$

From the Bayes' theorem (e.g., Papoulis, 1965, p. 177) it follows that

$$f_{H|D}(\eta | d) = f_{D|H}(d | \eta) f_H(\eta) / \int_0^\infty f_{D|H}(d | \eta) f_H(\eta) d\eta \quad (\text{A.30})$$

or

$$f_{HD}(\eta|d) = \varphi \eta e^{-\varphi \eta d} \frac{v^\alpha \eta^{\alpha-1} e^{-v \eta}}{\Gamma(\alpha)} / \int_0^\infty \varphi \eta e^{-\varphi \eta d} \frac{v^\alpha \eta^{\alpha-1} e^{-v \eta}}{\Gamma(\alpha)} d\eta \quad (\text{A.31})$$

which after algebraic manipulations becomes

$$f_{HD}(\eta|d) = \frac{(v + \varphi d)^{\alpha+1} \eta^\alpha e^{-(v + \varphi d) \eta}}{\Gamma(\alpha + 1)} \quad (\text{A.32})$$

This is the gamma probability density with shape parameter  $\alpha + 1$  and scale parameter  $v + \varphi d$ .

The mean of  $\Xi(t)$  conditional on  $D$  will be

$$E[\Xi(t)|D = d] = \int_0^\infty \{\kappa E[X] + (1 - \kappa) E[X] \exp(-\eta t)\} f_{HD}(\eta|d) d\eta \quad (\text{A.33})$$

which reduces to

$$E[\Xi(t)|D = d] = \kappa E[X] + (1 - \kappa) E[X] \left( \frac{v + \varphi d}{v + \varphi d + t} \right)^{\alpha+1} \quad (\text{A.34})$$

If we neglect the last term, which represents the boundary effect, we arrive at the same expression as in the original Bartlett-Lewis model.

The covariance function of  $\Xi(t)$  conditional on  $D$  will be

$$\begin{aligned} \text{Cov}[\Xi(t), \Xi(t + \tau)|D = d] = \\ \int_0^\infty \{\kappa E[X_i^2] \exp(-\eta \tau) + (1 - \kappa) E[X_i^2] \exp[-\eta(t + \tau)]\} f_{HD}(\eta|d) d\eta \end{aligned} \quad (\text{A.35})$$

which reduces to

$$\text{Cov}[\Xi(t), \Xi(t + \tau)|D = d] = \kappa E[X_i^2] \left( \frac{v + \varphi d}{v + \varphi d + \tau} \right)^{\alpha+1} + (1 - \kappa) E[X_i^2] \left( \frac{v + \varphi d}{v + \varphi d + t + \tau} \right)^{\alpha+1} \quad (\text{A.36})$$

If we neglect the last term, which represents the boundary effect, we get (17).

### A3. Expressions of variances and covariances in discrete time for the Bartlett-Lewis rectangular pulse model

It may be easily shown assuming a stationary process  $\Xi(t)$  that (A.3) results in

$$\text{Cov}[Y_i, Y_{i+m}] = \int_{-A}^A \text{Cov}[\Xi(t), \Xi(t+m\Delta + \tau)] (\Delta - |\tau|) d\tau \quad (\text{A.37})$$

Substituting the covariance term of the right-hand side of (A.37) from (16) we get for the original Bartlett-Lewis model

$$\text{Cov}[Y_i, Y_{i+m}] = \kappa E[X^2] \int_{-A}^A e^{-\eta |m\Delta + \tau|} (\Delta - |\tau|) d\tau \quad (\text{A.38})$$

which after algebraic calculations results in (20) when  $m > 0$  or in (19) when  $m = 0$ .

Similarly, substituting the covariance term of the right-hand side of (A.37) from (17) we get for the modified Bartlett-Lewis model

$$\text{Cov}[Y_i, Y_{i+m}] = \kappa E[X^2] \int_{-A}^A \left( \frac{v + \varphi d}{v + \varphi d + |m\Delta + \tau|} \right)^{\alpha+1} (\Delta - |\tau|) d\tau \quad (\text{A.39})$$

which after algebraic calculations results in (23) when  $m > 0$  or in (22) when  $m = 0$ .

### A4. Derivation of equation for the correction of rain depth variance at each class

Let  $\Omega$  denote the event that a storm's duration belongs to a certain class and  $\mu_D := E[D | \Omega]$ ,  $\sigma_D^2 := \text{Var}[D | \Omega]$ . Let also  $\mu'_H := E[H | \Omega]$  (the mean of the total storm depth when the storm's duration belong to the certain class),  $\mu_H := E[H | D = \mu_D]$  (the mean of the total storm depth when the storm's duration equals  $\mu_D$ ),  $\sigma_H^2 := \text{Var}[H | \Omega]$  and  $\sigma_H^2 := \text{Var}[H | D = \mu_D]$ . We need to estimate  $\mu_H$  and  $\sigma_H^2$  given  $\mu'_H$  and  $\sigma_H^2$ , which can be directly estimated from the available data.

We assume that each of the conditional moments  $E[H | D]$  and  $\text{Var}[H | D]$  is a power function of  $D$ , at least for durations in the certain class, i.e.,

$$E[H | D] = c_1 D^{1+\kappa_1} \quad (\text{A.40})$$

$$\text{Var}[H | D] = c_2 D^{2(1+\kappa_2)} \quad (\text{A.41})$$

where for generality we have assumed different  $\kappa$  in each case ( $\kappa_1$  and  $\kappa_2$ ). This assumption is true for the scaling model, with  $\kappa_1 = \kappa_2 = \kappa$ , and approximately valid for the BL model, in which case  $\kappa_1 = 0$  whereas  $\kappa_2 < 0$ . (As shown in Figure 4, the power relation for the variance of  $H$  approximately holds for the BL model as well). (A.40) and (A.41) can be written as

$$E[H | D] = \mu_H (D / \mu_D)^{1+\kappa_1} \quad (\text{A.42})$$

$$\text{Var}[H | D] = \sigma_H^2 (D / \mu_D)^{2(1+\kappa_2)} \quad (\text{A.43})$$

The mean  $\mu'_H$  is given by

$$\mu'_H = E[H | \Omega] = \int_{\zeta \in \Omega} E[H | \zeta] f_{D|\Omega}(\zeta) d\zeta = \int_{\zeta \in \Omega} \mu_H (D / \mu_D)^{1+\kappa_1} f_{D|\Omega}(\zeta) d\zeta \quad (\text{A.44})$$

where  $f_{D|\Omega}(\cdot)$  denotes the conditional probability density function of  $D$  in  $\Omega$ . To proceed with an approximation of  $\mu'_H$  we take the Taylor series of  $E[H | D]$  around  $D = \mu_D$ :

$$E[H | D] = \mu_H + (1 + \kappa_1)(D - \mu_D) (\mu_H / \mu_D) + (1/2) \kappa_1 (1 + \kappa_1) (D - \mu_D)^2 (\mu_H / \mu_D^2) + \dots \quad (\text{A.45})$$

Assuming that  $\kappa_1$  is small, the third term and all terms beyond can be neglected, so that

$$E[H | D] \approx \mu_H + (1 + \kappa_1)(D - \mu_D) (\mu_H / \mu_D) \quad (\text{A.46})$$

Substituting (A.46) into (A.44) and since

$$\int_{\zeta \in \Omega} f_{D|\Omega}(\zeta) d\zeta = 1, \quad \int_{\zeta \in \Omega} (D - \mu_D) f_{D|\Omega}(\zeta) d\zeta = 0 \quad (\text{A.47})$$

we get

$$\mu'_H \approx \mu_H \quad (\text{A.48})$$

which indicates that no correction is needed to obtain  $\mu_H$  from  $\mu'_H$ .

Similarly, we have

$$E[H^2 | D] = \sigma_H^2 (D / \mu_D)^{2(1+\kappa_2)} + \mu_H^2 (D / \mu_D)^{2(1+\kappa_1)} \quad (\text{A.49})$$

whose Taylor expansion around  $D = \mu_D$  is

$$\begin{aligned} E[H^2 | D] &= (\sigma_H^2 + \mu_H^2) + (2 / \mu_D) [(1 + \kappa_2) \sigma_H^2 + (1 + \kappa_1) \mu_H^2] (D - \mu_D) \\ &+ (1 / \mu_D^2) [(1 + \kappa_2) (1 + 2 \kappa_2) \sigma_H^2 + (1 + \kappa_1) (1 + 2 \kappa_1) \mu_H^2] (D - \mu_D)^2 + \\ &+ (2/3) (1 / \mu_D^3) [\kappa_2 (1 + \kappa_2) (1 + 2 \kappa_2) \sigma_H^2 + \kappa_1 (1 + \kappa_1) (1 + 2 \kappa_1) \mu_H^2] (D - \mu_D)^3 + \dots \end{aligned} \quad (\text{A.50})$$

Assuming that  $\kappa_1$  and  $\kappa_2$  are small, the fourth term and all terms beyond can be neglected, so that

$$\begin{aligned} E[H^2 | D] &\approx (\sigma_H^2 + \mu_H^2) + (2 / \mu_D) [(1 + \kappa_2) \sigma_H^2 + (1 + \kappa_1) \mu_H^2] (D - \mu_D) \\ &+ (1 / \mu_D^2) [(1 + \kappa_2) (1 + 2 \kappa_2) \sigma_H^2 + (1 + \kappa_1) (1 + 2 \kappa_1) \mu_H^2] (D - \mu_D)^2 \end{aligned} \quad (\text{A.51})$$

We note however that if  $\sigma_H^2 = 0$ , (A.51) results in

$$\begin{aligned} E[H^2 | D] &\approx \mu_H^2 + (2 / \mu_D) (1 + \kappa_1) \mu_H^2 (D - \mu_D) \\ &+ (1 / \mu_D^2) (1 + \kappa_1) (1 + 2 \kappa_1) \mu_H^2 (D - \mu_D)^2 \end{aligned} \quad (\text{A.52})$$

which is not consistent with (A.46). Indeed, in this special case  $\text{Var}[H | D] = 0$  and  $E[H^2 | D] = E^2[H | D]$ , which from (A.46) is

$$E[H^2 | D] \approx \mu_H^2 + (2 / \mu_D) (1 + \kappa_1) \mu_H^2 (D - \mu_D) + (1 / \mu_D^2) (1 + \kappa_1)^2 \mu_H^2 (D - \mu_D)^2 \quad (\text{A.53})$$

Thus, to make (A.51) consistent with (A.46), we replace  $(1 + 2 \kappa_2)$  and  $(1 + 2 \kappa_1)$  by  $(1 + \kappa_2)$  and  $(1 + \kappa_1)$ , respectively, so that it writes

$$\begin{aligned} E[H^2 | D] &\approx (\sigma_H^2 + \mu_H^2) + (2 / \mu_D) [(1 + \kappa_2) \sigma_H^2 + (1 + \kappa_1) \mu_H^2] (D - \mu_D) \\ &+ (1 / \mu_D^2) [(1 + \kappa_2)^2 \sigma_H^2 + (1 + \kappa_1)^2 \mu_H^2] (D - \mu_D)^2 \end{aligned} \quad (\text{A.54})$$

Besides



$$E[H^2 | \Omega] = \int_{\zeta \in \Omega} E[H^2 | \zeta] f_{D|\Omega}(\zeta) d\zeta \quad (\text{A.55})$$

which after substituting  $E[H^2 | \zeta]$  from (A.51) and also noticing that, in addition to (A.47),

$$\int_{\zeta \in \Omega} (D - \mu_D)^2 f_{D|\Omega}(\zeta) d\zeta = \sigma_D^2 \quad (\text{A.56})$$

yields

$$E[H^2 | \Omega] \approx (\sigma_H^2 + \mu_H^2) + (\sigma_D^2 / \mu_D^2) [(1 + \kappa_2)^2 \sigma_H^2 + (1 + \kappa_1)^2 \mu_H^2] \quad (\text{A.57})$$

Now, considering that  $\sigma_H'^2 = \text{Var}[H | \Omega] = E[H^2 | \Omega] - E^2[H | \Omega]$  and  $\mu_H' \approx \mu_H$ , we find that

$$\sigma_H'^2 \approx \sigma_H^2 + (\sigma_D^2 / \mu_D^2) [(1 + \kappa_2)^2 \sigma_H^2 + (1 + \kappa_1)^2 \mu_H^2] \quad (\text{A.58})$$

and solving for  $\sigma_H^2$

$$\sigma_H^2 \approx \frac{\sigma_H'^2 - \mu_H^2 (1 + \kappa_1)^2 \sigma_D^2 / \mu_D^2}{1 + (1 + \kappa_2)^2 \sigma_D^2 / \mu_D^2} \quad (\text{A.59})$$

If we set  $\kappa_1 = \kappa_2 = \kappa$  in (A.59) we find (26).

It may be shown that (A.59) is exact in the special case where  $H$  can be expressed as  $H = \Phi D$ , where  $\Phi$  is a random variable independent of  $D$ . In this case  $\kappa_1 = \kappa_2 = 0$ . In another special case where  $H$  can be expressed as the sum of  $D$  independent variables  $\Phi_i$  (assuming that  $D$  is integer), in which  $\kappa_1 = 0$  and  $\kappa_2 = -0.5$ , (A.59) would become exact if we omit the factor  $(1 + \kappa_2)^2$  in the denominator. Thus (A.59) becomes exact for both special cases if we slightly modify it to become

$$\sigma_H^2 \approx \frac{\sigma_H'^2 - \mu_H^2 (1 + \kappa_1)^2 \sigma_D^2 / \mu_D^2}{1 + [\max(0, 1 + 2\kappa_2)]^2 \sigma_D^2 / \mu_D^2} \quad (\text{A.60})$$

To verify (A.59) and (A.60) two series of stochastic simulations were performed. In the first one, for a given  $\kappa$ ,  $H$  was generated as  $H = \Phi D^{1 + \kappa}$ , where  $\Phi$  is a random variable independent of  $D$ , so that both (A.40) and (A.41) are valid for  $\kappa_1 = \kappa_2 = \kappa$ . In the second series,  $H$  was generated as the sum of  $D$  correlated variables  $\Phi_i$  (where  $D$  is integer), assuming that the sequence of  $\Phi_i$  is Markovian with mean  $\mu$  standard deviation  $\sigma$  and lag-one autocorrelation  $\rho > 0$ . It can be shown that in the second case,

$$E[H | D] = \mu D \quad (\text{A.61})$$

$$\text{Var}[H | D] = \sigma^2 \frac{D(1 - \rho^2) - 2\rho(1 - \rho^D)}{(1 - \rho)^2} \quad (\text{A.62})$$

Consequently,

$$\kappa_1 = \frac{d(\ln(E[H | D]))}{d(\ln D)} - 1 = 0 \quad (\text{A.63})$$

$$\kappa_2 = \frac{1}{2} \frac{d(\ln(\text{Var}[H | D]))}{d(\ln D)} - 1 = \frac{1}{2} + \rho \frac{1 - \rho^D(1 - D \ln \rho)}{D(1 - \rho^2) - 2\rho(1 - \rho^D)} \quad (\text{A.64})$$

Both (A.59) and (A.60) yielded good approximations in both series of simulations, even with large values of  $\sigma_D / \mu_D$ , which verifies their appropriateness.

## Tables

**Table 1** Characteristics of storms in Zographou meteorological station according to their duration (Time interval  $\Delta = 10$  min; durations in h, depths in mm).

Class	Class range		Number of storms	Duration		Storm depth		Incremental depth		
	$D_{\min}$	$D_{\max}$		$E[D]$	Std[ $D$ ]	$E[H]$	Std[ $H$ ]	$E[Y]$	Std[ $Y$ ]	Corr[ $Y_i, Y_{i+1}$ ]
1	0.17	2.00	19	1.09	0.65	12.99	5.09	1.95	3.18	0.39
2	2.17	4.00	14	2.95	0.53	18.27	13.07	1.03	1.87	0.43
3	4.17	12.00	18	7.67	2.64	23.49	13.60	0.51	1.28	0.63
4	12.17	18.00	17	14.90	1.75	36.34	17.84	0.41	0.88	0.58
5	18.17	40.00	13	24.78	6.91	60.55	38.68	0.41	1.11	0.60
A	0.50	5.00	38	2.28	1.35	16.63	12.26	1.24	2.39	0.51
B	5.17	40.00	43	16.08	1.47	39.50	29.02	0.41	1.01	0.58
All	0.17	40.00	81	9.57	8.85	28.77	25.37	0.50	1.26	0.57

**Table 2** Characteristics of storms in Zographou meteorological station according to their duration (Time interval  $\Delta = 1$  h; durations in h, depths in mm).

Class	Class range		Number of storms	Duration		Storm depth		Incremental depth		
	$D_{\min}$	$D_{\max}$		$E[D]$	Std[ $D$ ]	$E[H]$	Std[ $H$ ]	$E[Y]$	Std[ $Y$ ]	Corr[ $Y_i, Y_{i+1}$ ]
1	1	2	19	1.95	0.78	12.99	5.80	6.67	6.29	-0.30
2	3	4	14	3.86	0.77	18.27	13.04	4.74	6.03	0.02
3	5	12	18	8.50	2.60	23.49	13.74	2.76	4.93	0.25
4	13	18	17	15.88	1.80	36.34	17.85	2.29	3.45	0.42
5	19	40	13	25.46	6.79	60.55	38.78	2.38	4.61	0.55
A	1	5	38	3.11	1.47	16.63	12.26	5.36	6.65	0.10
B	6	40	43	16.91	7.40	39.50	28.02	2.34	4.07	0.45
All	1	40	81	10.43	8.82	28.77	25.37	2.76	4.64	0.38

**Table 3** Characteristics of storms in Parrish raingauge according to their duration (Time interval  $\Delta = 15$  min; durations in h, depths in mm).

Class	Class range		Number of storms	Duration		Storm depth		Incremental depth		
	$D_{\min}$	$D_{\max}$		$E[D]$	Std[ $D$ ]	$E[H]$	Std[ $H$ ]	$E[Y]$	Std[ $Y$ ]	Corr[ $Y_i, Y_{i+1}$ ]
1	0.25	0.25	608	0.25	0.00	3.40	1.30	3.40	1.30	–
2	0.50	0.50	139	0.50	0.00	10.10	5.60	5.10	3.70	0.23
3	0.75	0.75	113	0.75	0.00	15.60	9.70	5.20	4.70	0.32
4	1.00	1.00	78	1.00	0.00	20.10	13.00	5.00	5.20	0.32
5	1.25	1.50	112	1.38	0.13	18.40	12.77	3.40	4.00	0.39
6	1.75	2.25	109	1.98	0.23	21.20	14.75	2.70	3.80	0.40
7	2.50	3.25	107	2.83	0.28	25.10	17.76	2.20	3.90	0.50
8	3.50	4.50	137	3.98	0.38	26.90	19.76	1.70	3.40	0.49
9	4.75	7.00	119	5.73	0.73	28.80	20.52	1.30	3.00	0.49
10	7.25	26.75	121	12.08	4.83	47.00	27.44	1.00	2.10	0.35
A	1.00	4.00	491	2.17	0.96	22.40	15.79	2.58	3.99	0.45
B	4.25	26.75	292	8.12	4.60	35.70	26.25	1.10	2.51	0.44
All	0.25	26.75	1643	2.28	3.47	16.21	18.68	1.78	3.22	0.48

**Table 4** Characteristics of storms in Parrish raingauge according to their duration (Time interval  $\Delta = 2$  h; durations in h, depths in mm).

Class	Class range		Number of storms	Duration		Storm depth		Incremental depth		
	$D_{\min}$	$D_{\max}$		$E[D]$	Std[ $D$ ]	$E[H]$	Std[ $H$ ]	$E[Y]$	Std[ $Y$ ]	Corr[ $Y_i, Y_{i+1}$ ]
1	2	2	1124	2.00	0.00	9.30	10.30	9.30	10.30	–
2	4	4	227	4.00	0.00	25.50	17.70	12.70	13.70	0.02
3	6	6	132	6.00	0.00	26.70	21.20	8.90	13.00	0.08
4	8	8	64	8.00	0.00	31.60	19.30	7.90	10.60	0.07
5	10	10	35	10.00	0.00	35.10	19.70	7.00	9.00	0.27
6	12	14	27	12.80	1.00	47.70	26.04	7.50	9.10	0.09
7	16	28	34	19.60	4.00	69.10	30.98	7.10	8.80	0.26
A	8	12	52	10.60	0.95	37.40	19.79	7.02	8.57	0.12
B	14	28	44	18.20	4.17	66.45	32.02	7.27	9.12	0.23
All	2	28	1643	3.54	3.28	16.21	18.68	9.16	11.16	0.11

**Table 5** Fitted parameters of the scaling model of storm hyetograph.

Parameter	Zographou	Parrish
$\kappa$	–0.54	–0.60
$c_1$ (mm)	11.3	16.2
$c_2$ (mm <sup>2</sup> )	45.3	116.6
$\zeta$	0.92	0.00
$\beta$	0.21	0.34

**Table 6** Fitted parameters of the Bartlett-Lewis rectangular pulse model – original version.

Parameter	Zographou	Parrish
$\mu_X$ (mm h <sup>–1</sup> )	9.8	14.6
$\kappa$	0.53	0.97
$\eta$ (h <sup>–1</sup> )	4.83	6.36

**Table 7** Fitted parameters of the Bartlett-Lewis rectangular pulse model – random parameter version.

Parameter	Zographou	Parrish
$\mu_X$ (mm h <sup>-1</sup> )	9.2	15.3
$\kappa$	0.56	0.80
$\nu$ (h)	0.34	1.17
$\alpha$	2.02	7.86
$\varphi$	0.0157	0.0001

**Table 8** Fitted parameters of the Bartlett-Lewis rectangular pulse model – additional version.

Parameter	Zographou	Parrish
$\mu_X$ (mm h <sup>-1</sup> )	13.1	16.5
$\kappa_0$	0.86	0.98
$\kappa_1$	-0.54	-0.60
$\eta_0$ (h <sup>-1</sup> )	7.92	8.24
$\eta_1$	-0.33	-0.34

## List of Figures

**Figure 1** Explanatory sketch for the scaling model of storm hyetograph.

**Figure 2** Explanatory sketch for the Bartlett-Lewis rectangular pulse model.

**Figure 3** Empirical and theoretical mean of total storm depth as a function of storm duration: (a) Zographou,  $\Delta = 10$  min; (b) Zographou,  $\Delta = 1$  h; (c) Parrish,  $\Delta = 15$  min; (d) Parrish,  $\Delta = 2$  h.

**Figure 4** Empirical and theoretical standard deviation of total storm depth as a function of storm duration: (a) Zographou,  $\Delta = 10$  min; (b) Zographou,  $\Delta = 1$  h; (c) Parrish,  $\Delta = 15$  min; (d) Parrish,  $\Delta = 2$  h.

**Figure 5** Empirical and theoretical mean of incremental storm depth as a function of storm duration: (a) Zographou,  $\Delta = 10$  min; (b) Zographou,  $\Delta = 1$  h; (c) Parrish,  $\Delta = 15$  min; (d) Parrish,  $\Delta = 2$  h.

**Figure 6** Empirical and theoretical standard deviation of incremental storm depth as a function of storm duration: (a) Zographou,  $\Delta = 10$  min; (b) Zographou,  $\Delta = 1$  h; (c) Parrish,  $\Delta = 15$  min; (d) Parrish,  $\Delta = 2$  h.

**Figure 7** Empirical and theoretical lag-one autocorrelation coefficient of incremental storm depth as a function of storm duration: (a) Zographou,  $\Delta = 10$  min; (b) Zographou,  $\Delta = 1$  h; (c) Parrish,  $\Delta = 15$  min; (d) Parrish,  $\Delta = 2$  h.

**Figure 8** Empirical and theoretical autocorrelation function of incremental storm depth for small storm durations: (a) Zographou,  $\Delta = 10$  min; (b) Zographou,  $\Delta = 1$  h; (c) Parrish,  $\Delta = 15$  min; (d) Parrish,  $\Delta = 2$  h.

**Figure 9** Empirical and theoretical autocorrelation function of incremental storm depth for large storm durations: (a) Zographou,  $\Delta = 10$  min; (b) Zographou,  $\Delta = 1$  h; (c) Parrish,  $\Delta = 15$  min; (d) Parrish,  $\Delta = 2$  h.



## Figures

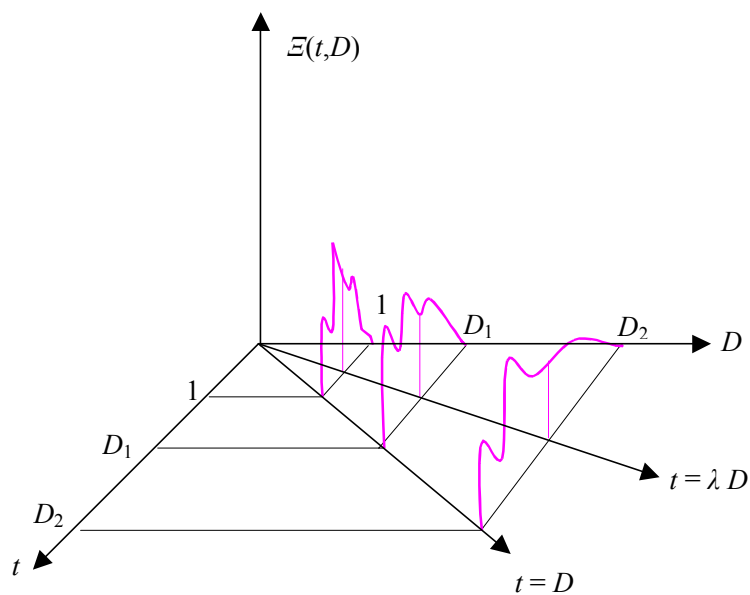


**Figure 1** Explanatory sketch for the scaling model of storm hyetograph.

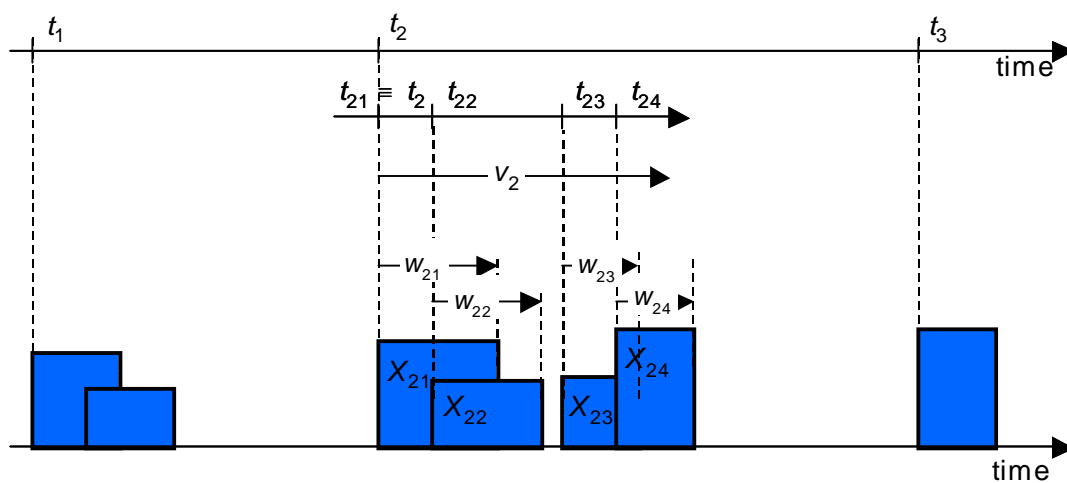


**Figure 2** Explanatory sketch for the Bartlett-Lewis rectangular pulse model.

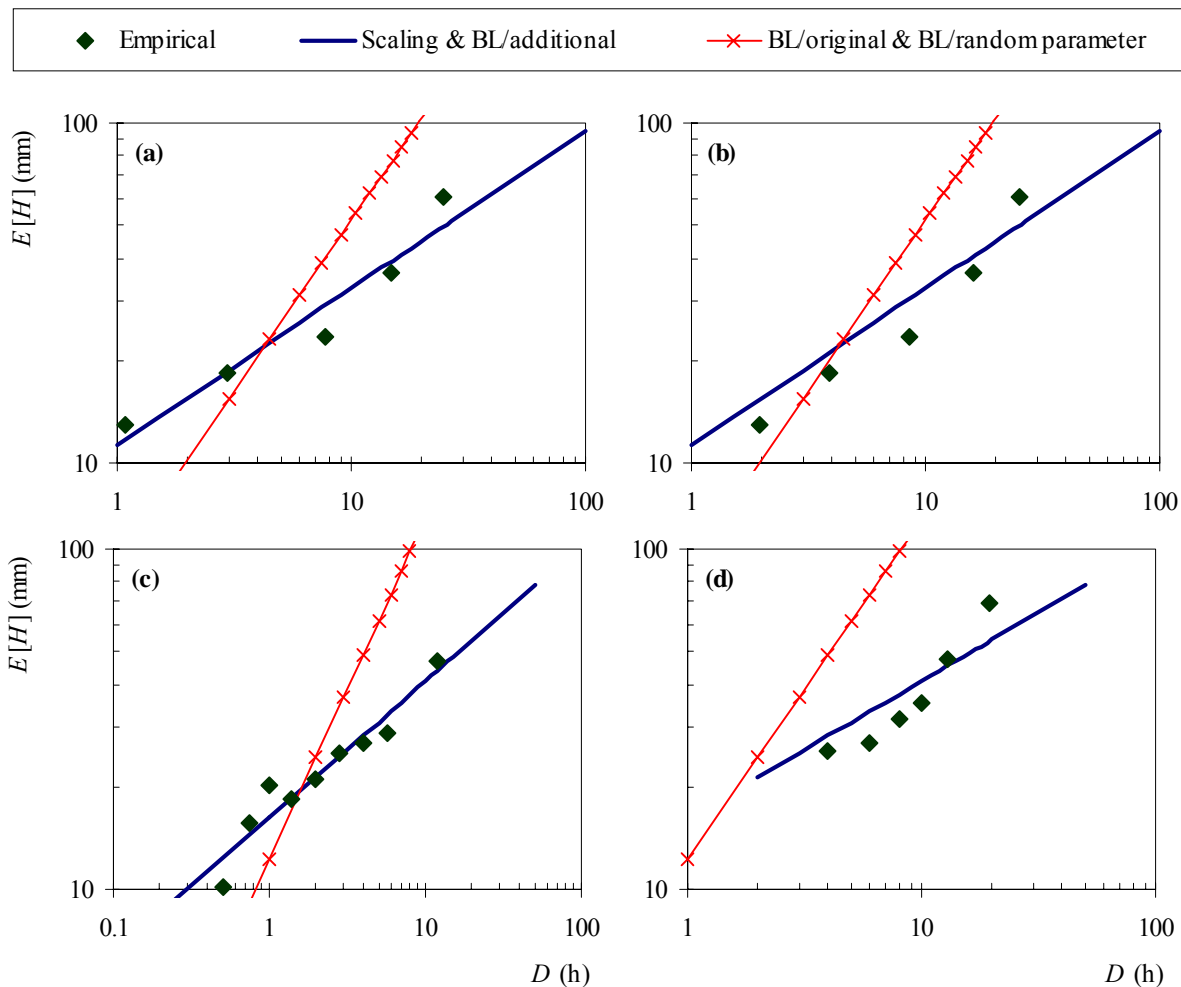


**Figure 3** Empirical and theoretical mean of total storm depth as a function of storm duration: (a) Zographou,  $\Delta = 10$  min; (b) Zographou,  $\Delta = 1$  h; (c) Parrish,  $\Delta = 15$  min; (d) Parrish,  $\Delta = 2$  h.

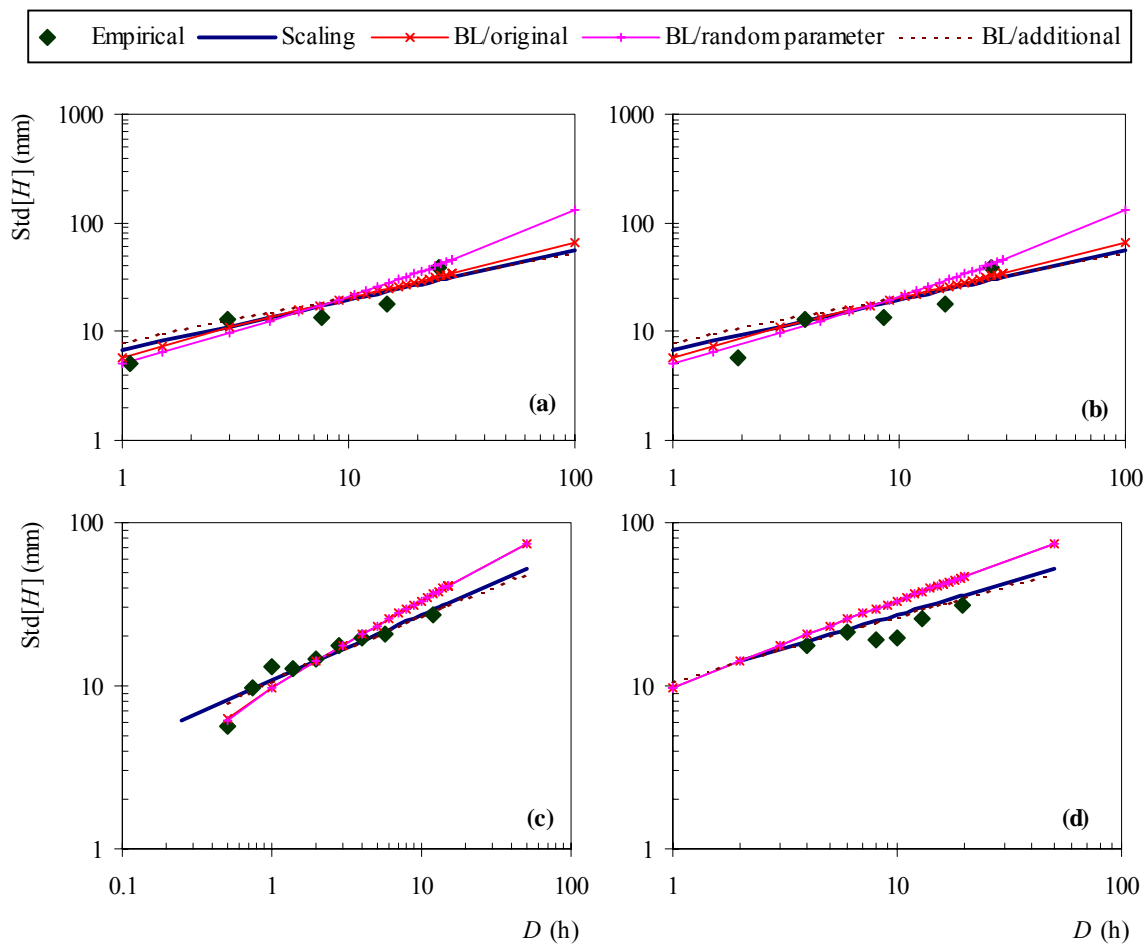


**Figure 4** Empirical and theoretical standard deviation of total storm depth as a function of storm duration: (a) Zographou,  $\Delta = 10$  min; (b) Zographou,  $\Delta = 1$  h; (c) Parrish,  $\Delta = 15$  min; (d) Parrish,  $\Delta = 2$  h.

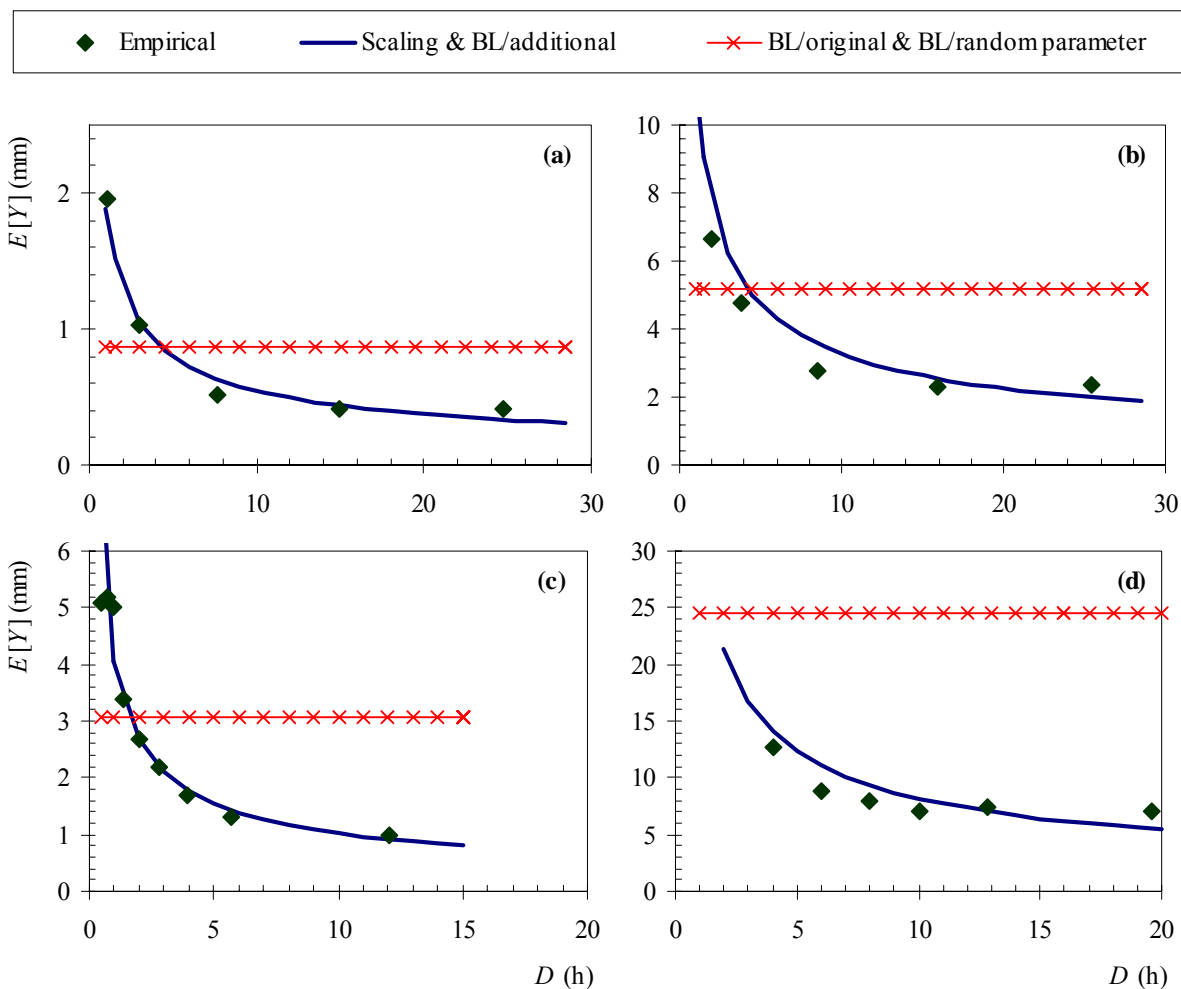


**Figure 5** Empirical and theoretical mean of incremental storm depth as a function of storm duration: (a) Zographou,  $\Delta = 10$  min; (b) Zographou,  $\Delta = 1$  h; (c) Parrish,  $\Delta = 15$  min; (d) Parrish,  $\Delta = 2$  h.

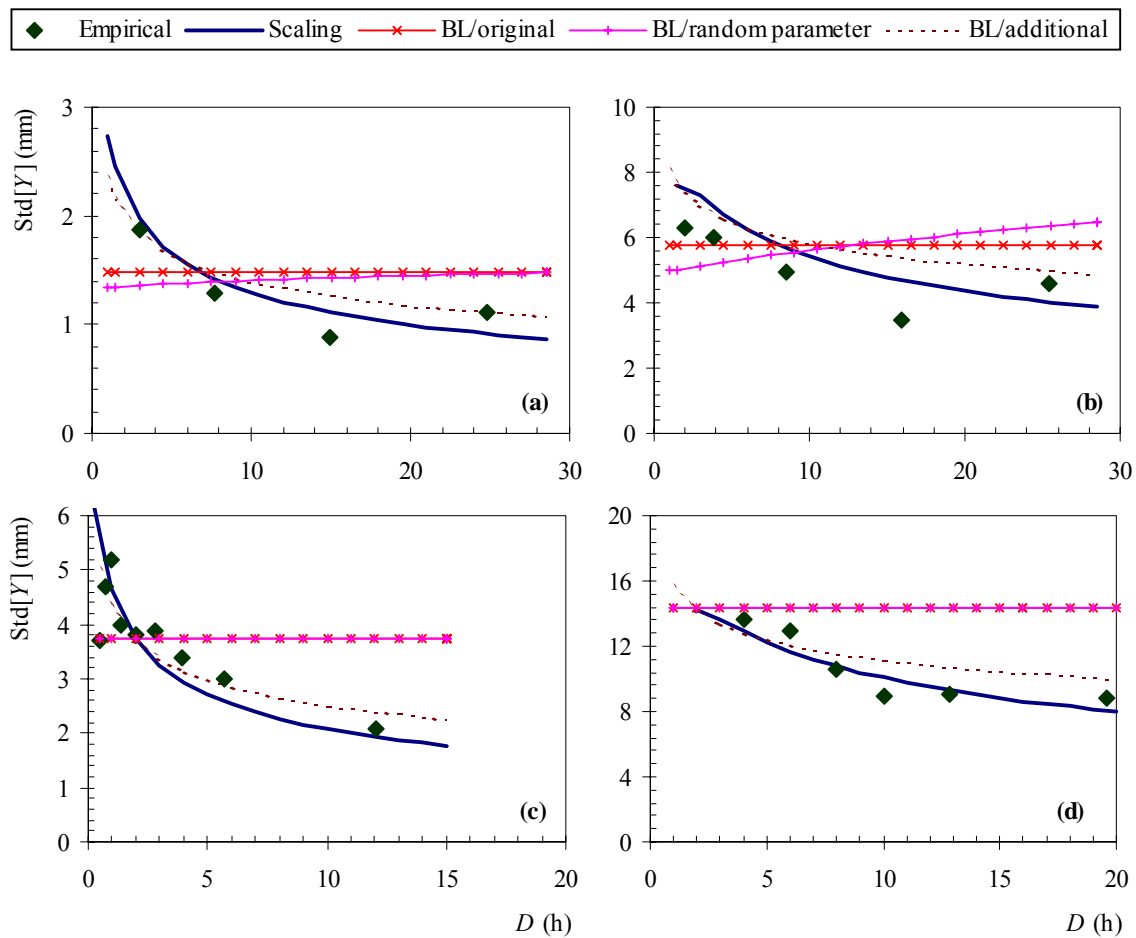


**Figure 6** Empirical and theoretical standard deviation of incremental storm depth as a function of storm duration: (a) Zographou,  $\Delta = 10$  min; (b) Zographou,  $\Delta = 1$  h; (c) Parrish,  $\Delta = 15$  min; (d) Parrish,  $\Delta = 2$  h.

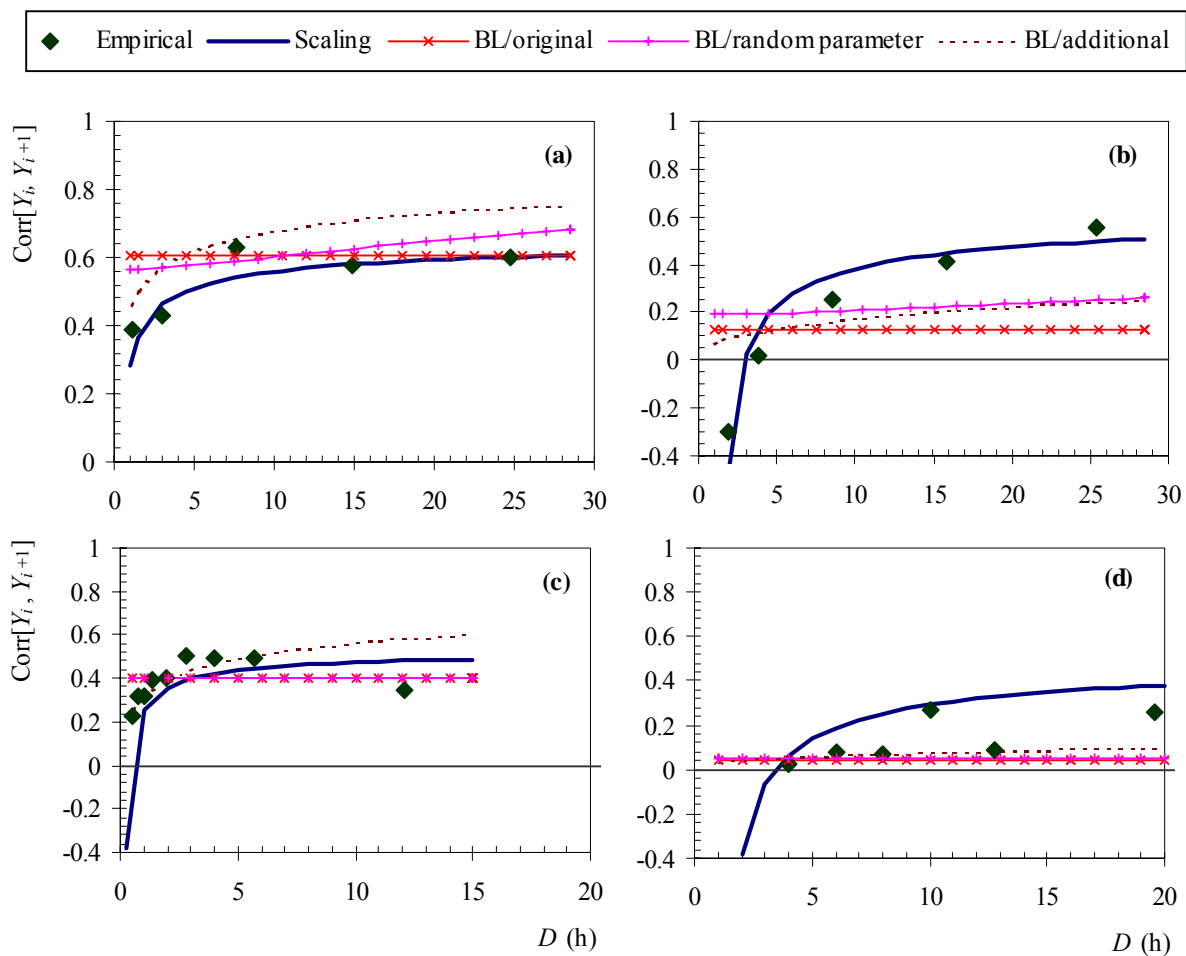


**Figure 7** Empirical and theoretical lag-one autocorrelation coefficient of incremental storm depth as a function of storm duration: (a) Zographou,  $\Delta = 10$  min; (b) Zographou,  $\Delta = 1$  h; (c) Parrish,  $\Delta = 15$  min; (d) Parrish,  $\Delta = 2$  h.

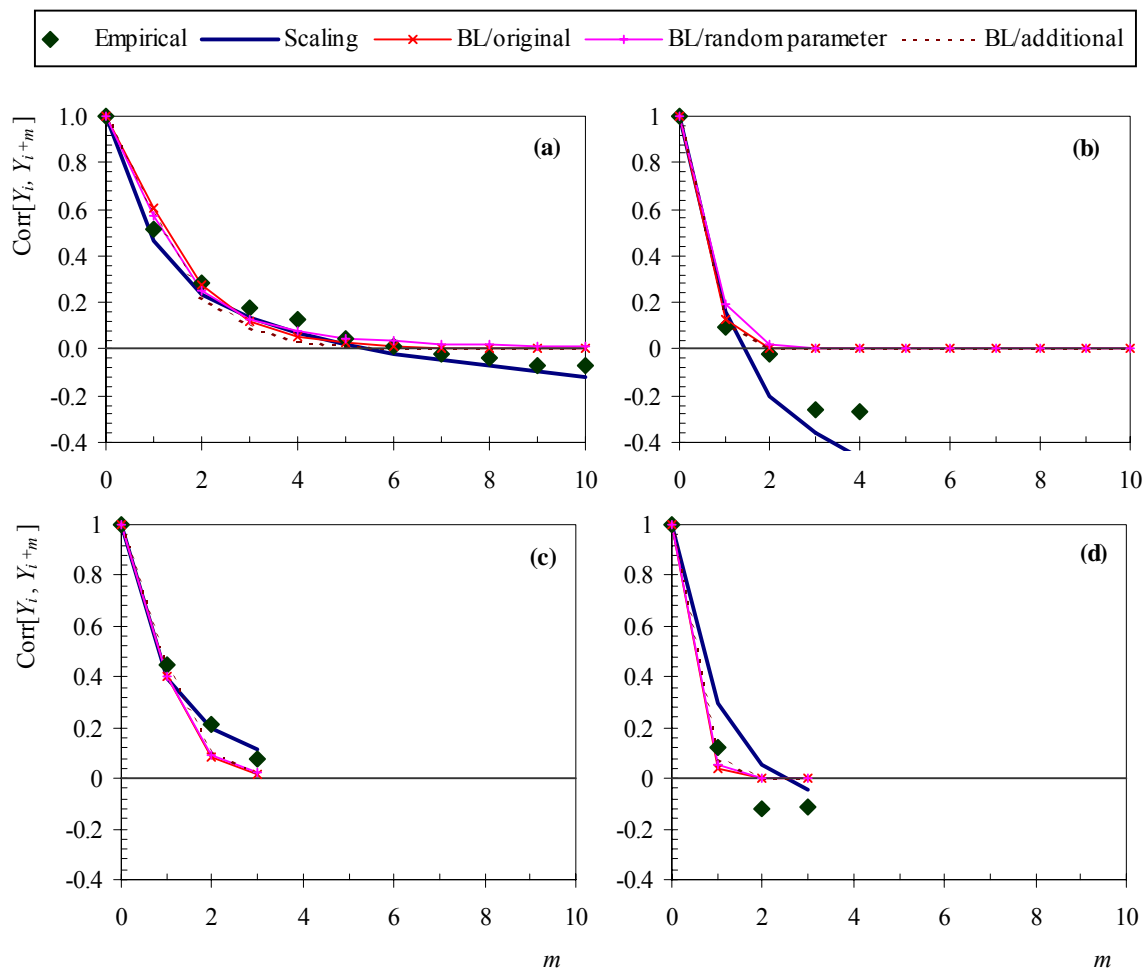


**Figure 8** Empirical and theoretical autocorrelation function of incremental storm depth for small storm durations: (a) Zographou,  $\Delta = 10$  min; (b) Zographou,  $\Delta = 1$  h; (c) Parrish,  $\Delta = 15$  min; (d) Parrish,  $\Delta = 2$  h.

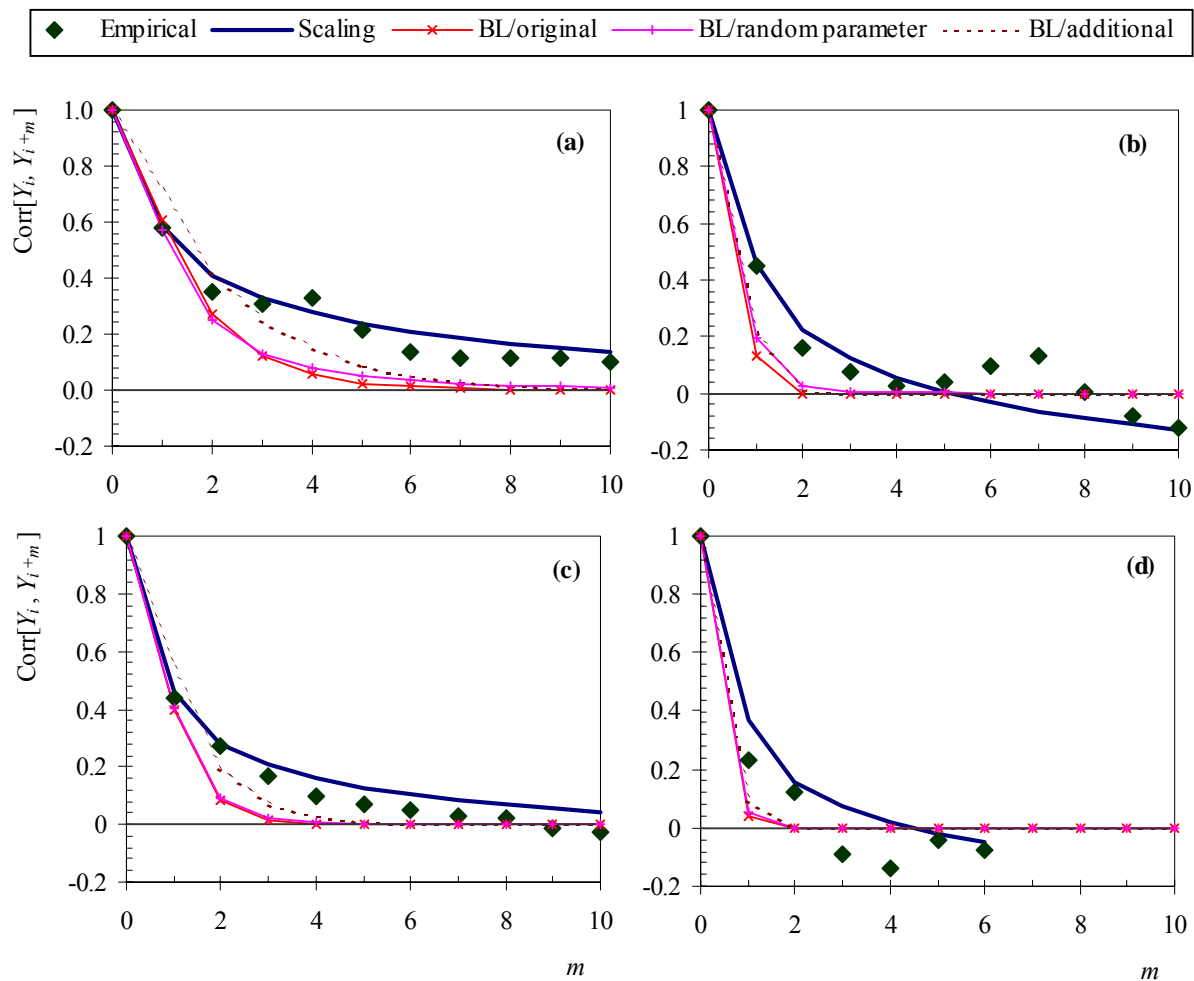


**Figure 9** Empirical and theoretical autocorrelation function of incremental storm depth for large storm durations: (a) Zographou,  $\Delta = 10$  min; (b) Zographou,  $\Delta = 1$  h; (c) Parrish,  $\Delta = 15$  min; (d) Parrish,  $\Delta = 2$  h.